Supplementary Information

A Carbonate-Forming Baeyer-Villiger Monooxygenase

Youcai Hu[1], David Dietrich[2], Wei Xu[1], Ashay Patel[3], Justin A. J. Thuss[2], Jingjing Wang[1], Wen-Bing Yin[1], Kangjian Qiao[1], Kendall N. Houk[3], John C. Vederas[2], Yi Tang[1,3]

[1]Department of Chemical and Biomolecular Engineering, [3]Department of Chemistry and Biochemistry, University of California, Los Angeles, Los Angeles, CA 90095 (USA)
[2]Department of Chemistry, University of Alberta, Edmonton, Alberta, T6G 2G2, Canada
E-mail: yitang@ucla.edu, john.vederas@ualberta.ca

TABLE OF CONTENTS

Supplementary Results

Supplementary Tables

Supplementary Table 1. 1D and 2D NMR data of ketocytochalasin (**7**) in $CDCl_3$ (500 MHz for ^1H NMR and 125 MHz for ^{13}C NMR)

no.	δ_H, mult. (*J* in Hz)	δ_C	COSY	HMBC
1'		137.4		
2', 6'	7.11, d (7.4)	129.1	H-3', H-5'	C-4', C-2'/C-6', C10
3', 5'	7.28, m	128.8	H2', H-4', H-6'	C-1', C-5'/C-3'
4'	7.23, dd (7.4, 7.4)	126.9	H-3', H-5'	C-2'/C-6'
1		173.4		
3	3.22, m	54.8	H-10a, H-10b, H-4	C-1, C-9
4	3.23, m	47.7	H-3	C-21, C-6, C11,C-1, C-10, C-5
5	2.37, m	34.7	H-11, H-4	C3,C4, C6, C11
6		140.4		
7	5.43, d (13.9)	125.2	H-8	C5,C7,C8, C12,C13
8	2.47, m	49.4	H-12, H-13, H-7	C4,C6,C7,C21
9		68.9		
10a	2.78, m	45.0	H-3	C3, C4, C1', C2', C6'
10b	2.53, m		H-3	C3, C4, C1', C2', C6'
11	1.14, d (7.2)	13.5	H-5	C6, C4, C5
12	1.73, br s	20.0		C6, C7, C5
13	5.95,dd d(15.6, 10.0, 2.3)	130.0	H-8, H-14	C-15, C-7, C-8
14	4.97, ddd (15.6, 11.0, 4.5)	133.7	H-13, H-8, H-15a, H-15b	C15, C-8
15a	2.53, m	37.6	H-14, H-15b, H-16	C13, C14,C16,C17
15b	1.98, m		H-14, H-15a	C13, C14,C16,C17, C22
16	2.58, m	43.7	H-15a, H-22	C14,C15,C17, C22
17		210.2		
18	3.38, m	50.9	H-19, 1.40	C17, C19, C20, C23, C16
19	6.09, dd (16.1, 6.5)	139.2	H-20, H-18	C17, C18, C20, C21, C23
20	7.02, d (16.1)	135.2	H-19	C21, C18
21		196.8		
22	1.16, d (7.1)	19.9	H-16	C15, C16, C17
23	1.41, d (7.2)	15.6	H-18	C17, C18, C19
2-NH	5.68, brs			C1, C3, C4, C9

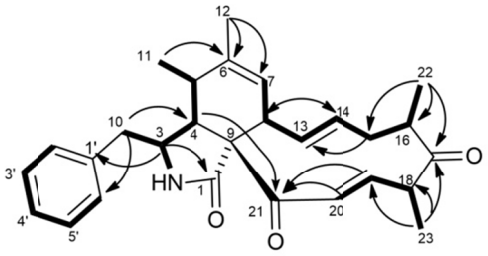

ketocytochalasin (**7**)

^1H, ^1H-COSY → HMBC

Supplementary Table 2: NMR data of cytochalasin Z_{16} (**9**) and cytochalasin E (**1**) in $CDCl_3$(500 MHz for ^1H NMR and 125 MHz for ^{13}C NMR)

no.	**9**				**1**	
	δ_H, mult. (*J* in Hz) [a]	δ_C [a]	δ_H, mult. (*J* in Hz) [b]	δ_C [b]	δ_H, mult. (*J* in Hz)	δ_C
1’		137.9		137.8		135.8
2’, 6’	7.17, d (7.2)	129.1	7.17, d (7.0)	129.0	7.16, d (7.2)	129.7
3’, 5’	7.31, dd (7.2, 7.2)	129.0	7.31, dd (7.2, 7.2)	129.0	7.32, dd (7.2, 7.2)	128.9
4’	7.24, (7.2)	127.0	7.24, t (7.3, 7.3)	127.0	7.27, t (7.2, 7.2)	127.3
1		170.2		170.1		170.5
3	3.04, m	56.2	3.03-3.06, m	56.2	3.78r s, b	53.3
4	2.89, m	50.9	2.90-2.93, m	50.8	3.03, m	47.7
5	2.67-2.72, m	34.5	2.67-2.72, m	34.5	2.27, m	35.8
6	-	140.9		140.8		57.3
7	5.44, m	122.7	5.37, brs	122.7	2.67, m	60.6
8	2.90-2.92, m	47.7	2.90-2.93, m	47.7	2.64, m	45.8
9		89.0		89.0		87.2
10	3.05, m	43.3	3.05-3.08, m	43.3	2.90, dd (13.5, 5.0)	44.6
	2.91, m		2.90-2.92, m		2.72, dd (13.5, 7.0)	
11	1.26, d (7.5)	14.4	1.26, d (7.3)	14.3	1.07, d (7.8)	13.1
12	1.78, brs	20.1	1.78, brs	20.1	1.26, s	20.0
13	5.67, ddd (15.1, 9.9, 1.6)	129.4	5.67, dd (15.4, 9.9)	129.4	5.89, dd (15.1, 8.0)	128.5
14	5.46, ddd (15.1, 9.9, 4.6)	131.2	5.46, ddd (14.6, 9.9, 4.4)	131.8	5.22, dd (15.1, 8.0)	131.5
15a	2.69, m	34.5	2.69-2.71, m	34.5	2.64, m	39.1
15b	2.12, m		2.12, ddd (14.0, 9.9, 6.2)		2.15, m	
16	2.61, m	46.1	2.60-2.63, m	46.0	2.90, m	40.8
17		212.7		212.7		211.7
18	3.36, dq (8.1, 6.6)	40.2	3.36, dq (8.1, 6.6)	40.3		76.7
19	5.62, dd (12.4, 8.4)	116.5	5.62, dd (12.4, 8.4)	116.5	5.59, d (12.2)	120.4
20	6.42, dd (12.2, 0.8)	140.2	6.42, d (12.2)	140.2	6.43, d (12.2)	142.0
21		149.8		149.8		149.3
22	1.30, d (7.3)	16.3	1.30, d (7.3)	16.3	1.14, d (7.0)	19.7
23	1.20, d (6.9)	17.4	1.21, d (7.0)	17.4	1.46, s	24.3

a: measured in this study (^1H 500 MHz, ^{13}C 125 MHz); b: reported value in reference[1]

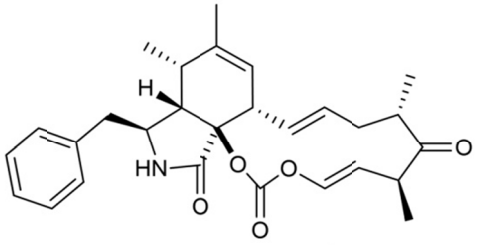

Cytochalasin Z_{16} (**9**)

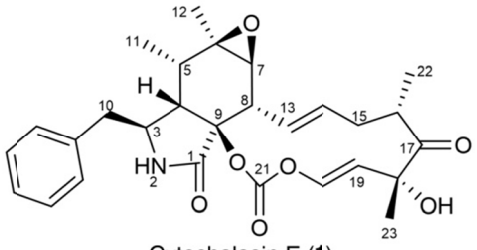

Cytochalasin E (**1**)

Supplementary Table 3: NMR data of iso-precytochalasin (**8**) and rosellichalasin (**5**) in $CDCl_3$(500 MHz for ^1H NMR and 125 MHz for ^{13}C NMR)

no.	**8**				**5**	
	δ_H, mult. (*J* in Hz)	δ_C	COSY	HMBC	δ_H, mult. (*J* in Hz)	δ_C
1'		137.8				136.6
2', 6'	7.18, d (7.2)	129.1	H3'H/5'	C4', C6'/C2', C10	7.18, d (7.2)	129.4
3', 5'	7.31, dd (7.4, 7.4)	128.9	H2'/H6', H4'	C1', C3'/C5'	7.34, dd (7.2, 7.2)	128.8
4'	7.27, d (7.2)	127.0		C2', C6'	7.28, d (7.2)	125.6
1		174.3				169.0
3	3.08, m	55.8	H4, H10		3.68, t (6.8)	53.7
4	2.62, dd (4.1, 4.1)	51.6	H3, H5		2.71, d (5.4)	49.1
5	2.76, m	34.5	H4, H7, H11		2.23, m	35.9
6		140.3				57.0
7	5.33, brs	123.3	H5, H8, H12		2.67, d (5.4)	60.1
8	3.07, m	47.2	H7, H13		2.88, dd (10.3, 5.4)	46.9
9		86.6		-		84.4
10	2.88, d (8.6)	43.9	H3	C3, C1', C2'/C6'	2.85, d (6.4)	44.2
11	1.22, d (7.2)	14.1	H5	C6, C4, C5	1.05, d (6.8)	12.7
12	1.73, br s	20.3	H7	C6, C7, C5	1.22, s	19.5
13	5.60, ddd (15.0, 9.8, 1.8)	127.3	H8, H14		5.83, dd (15.2, 10.3)	127.1
14	5.48 ddt (15.0, 10.9, 3.6)	133.9	H13, H15		5.46, ddt(15.2, 10.3, 4.2)	131.5
15α	2.22 ,m	39.7	H16, H14		2.24, m	36.4
15β	2.09, m		H16		2.04, dd(11.7, 11.7)	
16	3.33, m	39.5	H15, H22		3.27,m	39.7
17		204.6				205.3
18		143.3				143.0
19	6.55, t (8.0)	132.5	H20, H23	C17, C23	6.34, t (8.0)	135.2
20α	3.27, m	36.1	H19	C21, C18, C19	2.98, dd (12.1, 7.1)	39.6
20β	3.20, m		H19	C21, C19	3.25, m	
21		170.6				171.3
22	1.14, d (6.8)	17.9	H16	C17, C15	1.12, d (6.8)	17.3
23	1.85, s	12.3		C17, C18, C19	1.85, br s	12.8
2-NH	5.40, br s			C4, C9	5.99, br s	-

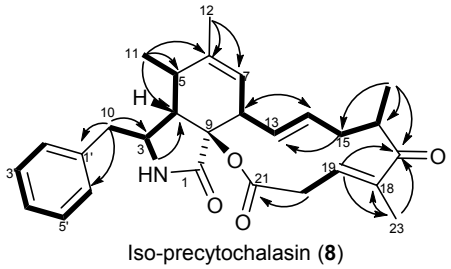

Iso-precytochalasin (**8**)

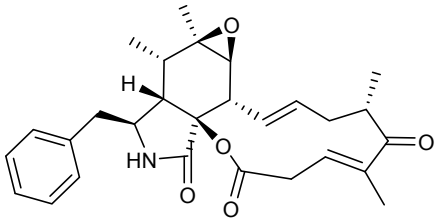

rosellichalasin (**5**)

^1H, ^1H-COSY ⟶ HMBC

Supplementary Table 4: NMR data of dehydrozygosporin D **(12)** in $CDCl_3$ (500 MHz for ^1H NMR and 125 MHz for ^{13}C NMR)

no.	δ_H, mult. (*J* in Hz)	δ_C
1'		137.0
2', 6'	7.35, m	128.9
3', 5'	7.16, m	129.2
4'	7.25-7.23, m	127.0
1		172.7
3	3.29, m	53.1
4	3.24, dd (5.9, 2.4)	45.2
5	2.77, m	31.6
6		148.5
7	4.06, d (10.1)	71.5
8	2.41, dd (9.9, 9.9)	51.7
9		64.1
10	2.67, dd (13.4, 5.5)	44.2
11	1.00, d (6.7)	13.0
12a	5.25, s	114.4
12b	5.08, s	114.4
13	5.80, ddd (15.5, 9.8, 0.9)	129.8
14	5.19, ddd (15.5, 10.9, 4.7)	135.0
15a	2.57, dt (13.1, 11.0)	38.3
15b	2.12-2.07, m	38.3
16	2.72, ddd (10.9, 6.8, 1.3)	42.9
17		209.9
18		78.6
19	6.35, d (15.7)	143.3
20	6.97, d (15.7)	134.3
21		197.4
22	1.19, d (7.72)	19.8
23	1.62, s	23.6

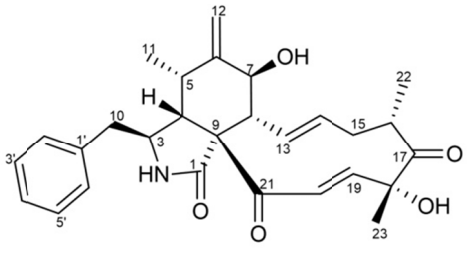

dehydrozygosporin D (**12**)

Supplementary Table 5. Sequences of primers used in the construction of plasmids.

Primers	*Sequences*
Lig4KO-1	5'-CGTTATGCAGCCCGATATCA -3'
Lig4KO-2	5'-ATGGGCGTGGGAGACATCTG -3'
Lig4KO-3	5'-AGCCGGTGGAGCGGCGTCGACGAAAAGGGGTTTCTCTGTTCA -3'
Lig4KO-4	5'-GTCCGAGGGCAAAGGAATGAGTTTAGCGTGGACAATTTTCGTC -3'
Lig4KO-5	5'-CCTTTTCTCACATCATCATGAACTTG-3'
Lig4KO-6	5'-CGCAAATTACGACTACGACTACAAC -3'
Lig4KO-7	5'-ACGCCGCTCCACCGG -3'
Lig4KO-8	5'-CATATGAAATCACGCCATGTAGTG -3'
Lig4KO-9	5'-GCCAATACCCCATACCACCTC -3'
Lig4KO-10	5'-TCATTCCTTTGCCCTCGGAC -3'
ccsBKO-1	5'-GATCCCTCTTTCGGATCTTAGGGGC -3'
ccsBKO-2	5'AGGGAACAAAAGCTGGAGCTCGGATCCATTTAGCAATGGGTGTTGCGCGCAGAA-3'
ccsBKO-3	5'-CGCCCCGTCCGGTCCTGCCCGTCACCGAGATTTAGGGGGTGCGTTGGAAAACGT-3'
BAR-4	5'-CTAAATCTCGGTGACGGGCAGGA -3'
BAR-5	5'-CGACAGAAGATGATATTGAAGGAGC -3'
ccsBKO-6	5'-CCCAAAAAGTGCTCCTTCAATATCATCTTCTGTCGTCTTGCGTAGGACGGTATATT-3'
ccsBKO-7	5'-ACGTTGTAAAACGACGGCCAGTGAATTCGAGCTCGAACGGAGCTTTTGGCGTCG-3'
ccsBKO-8	5'-CGCTCACAAGGCTCAAGGGC-3'
ccsB-f	5'-AA*CATATG*GATTATAAGGATGATGATGATAAGCTGCAAACGCTTCAATTCGACAAG-3'
ccsB-r	5'-AA*GCGGCCGC*TCAGCGCTTGTCCATTCCCTG-3'
ccsB-R421A	5'-GCCCTGGTACTCGTTCATGTGCAAA**gc**ACCGACGTTTCACAATGACTAC-3'

Supplementary Table 6. *Aspergillus clavatus* strains used in this study

Strain	*Genotype*	*Reference*
A. clavatus NRRL1	Parental cytochalasin E/K producer	Fedorova et al., 2008 [2]
A. clavatus Δlig4	*Δ lig4*	This work
A. clavatus OE*:ccsR, Δlig4*	*ccsR* overexpressed, *Δlig4*	This work
A. clavatus OE*:ccsR, Δlig4, ΔccsB* (*ΔccsB*-37)	*ccsR* overexpressed, *Δlig4, ΔccsB*	This work

Supplementary Table 7. Expression plasmids used in this study

Plasmid	**Vector Source**	**Genes**	**Marker**	**Reference**
pYC01	pET23a	*ccsB*	*Amp*	This work
pYC04	pET23a	*ccsB R421A mutant*	*Amp*	This work

Supplementary Figures

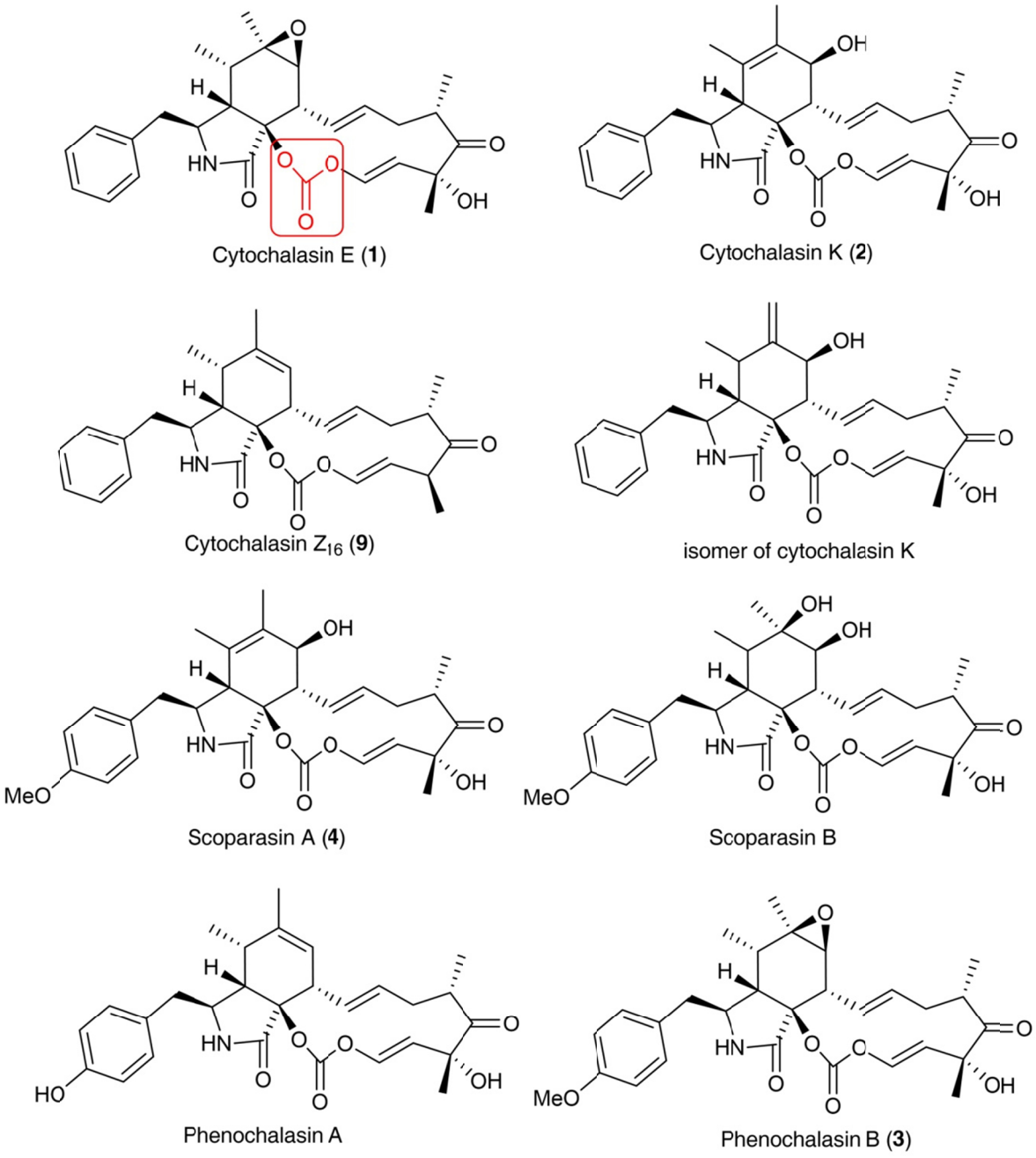

Supplementary Figure 1. All natural cytochalasins with carbonate moiety[3-7]. Although total syntheses of numerous members of the family have been completed[8-11], no synthesis of the carbonate containing members has been reported to date, likely due to the presence of the challenging carbonate group.

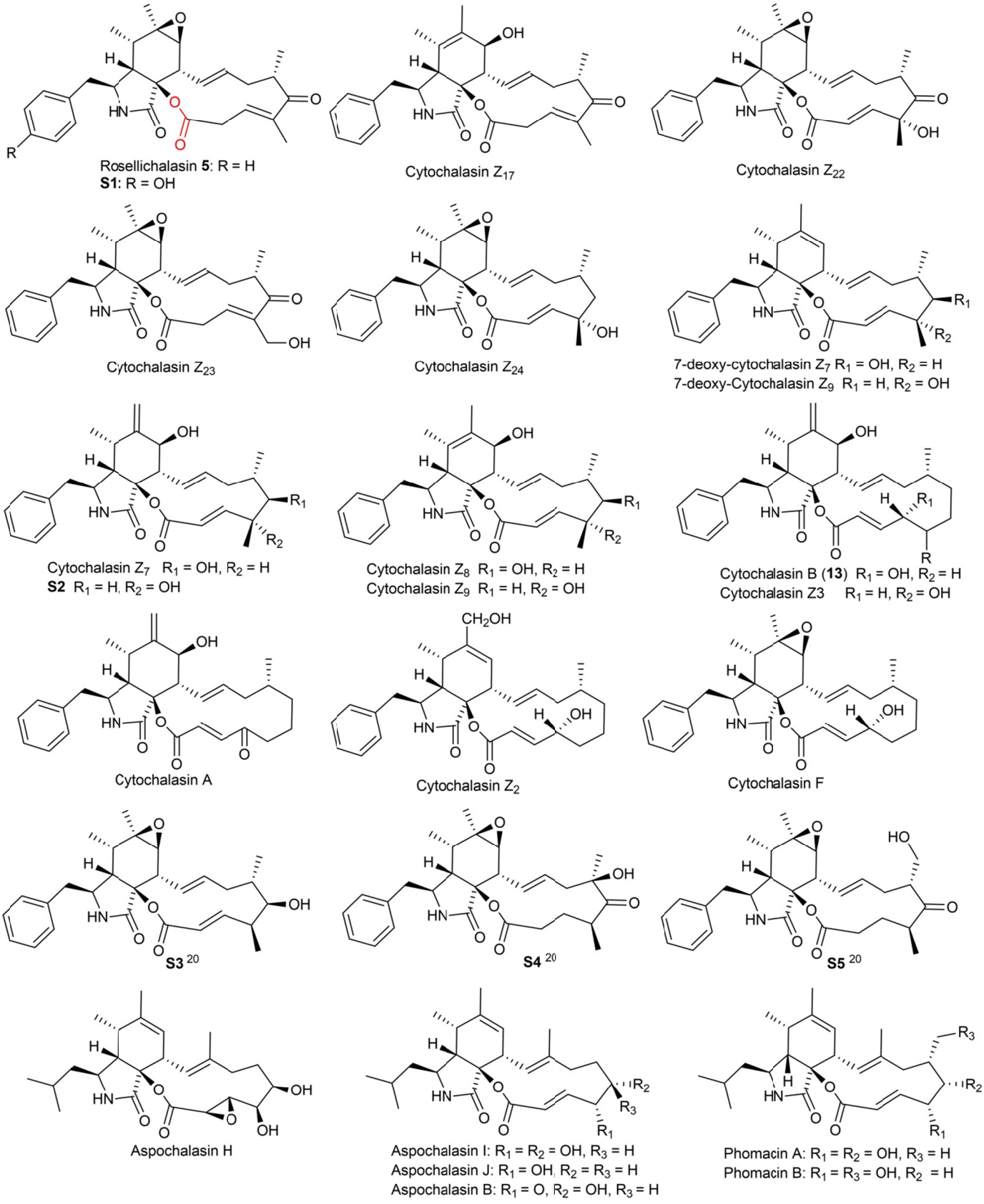

Supplementary Figure 2. Examples of natural cytochalasins containing lactone moiety [1, 12-21]

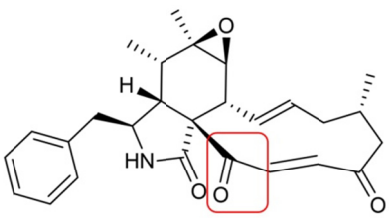

Cytcchalasin G (**6**)

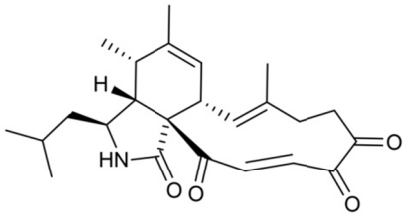

Aspochalasin A

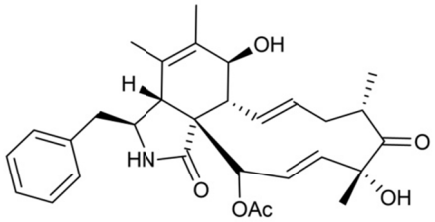

Cytochalasin C

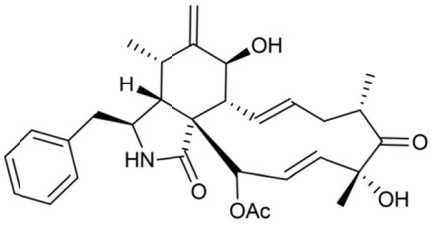

Cytochalasin D

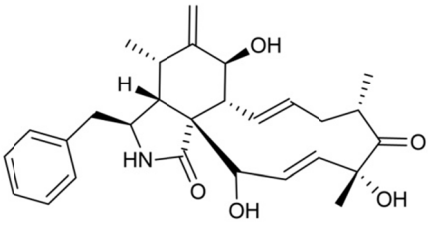

Zygosporin D

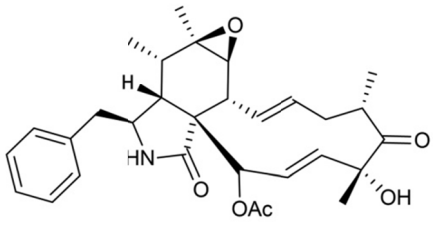

Cytochalasin Q

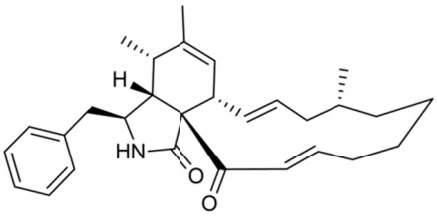

Proxiphomin

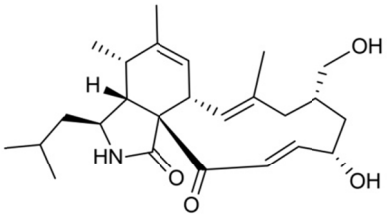

Phomacin C

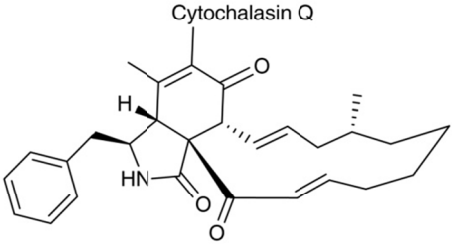

Protophomin

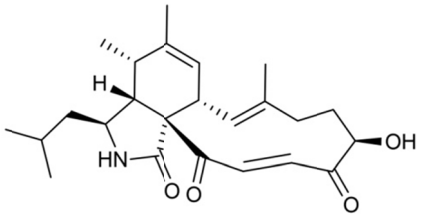

Aspochalasin B

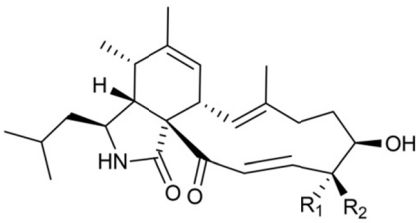

Aspochalasin C R_1 = H, R_2 = OH
Aspochalasin D R_1 = OH, R_2 = H

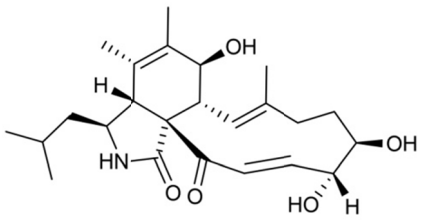

Aspochalasin U

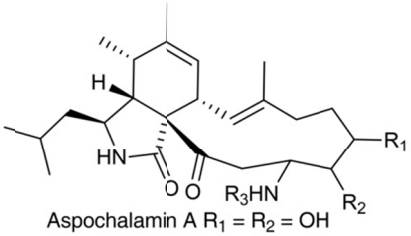

Aspochalamin A R_1 = R_2 = OH
Aspochalamin B R_1 = R_2 = OH
Aspochalamin C R_1 = R_2 = OH
Aspochalamin D R_1 = R_2 = H

R_3 =

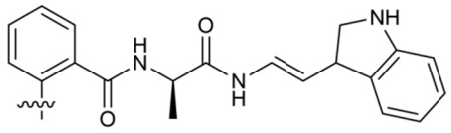

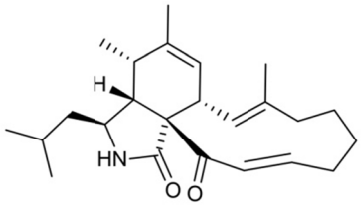

Aspochalasin Z

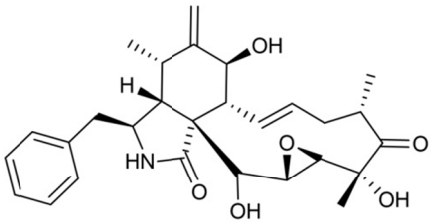

Engleromycin

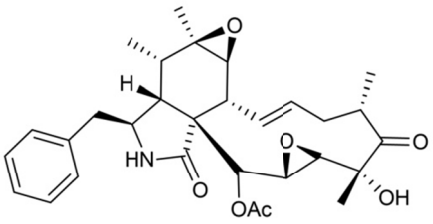

19,20-epoxycytochalasin Q

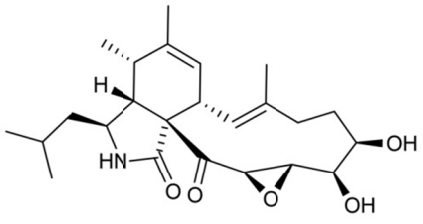

Aspochalasin H

continue...

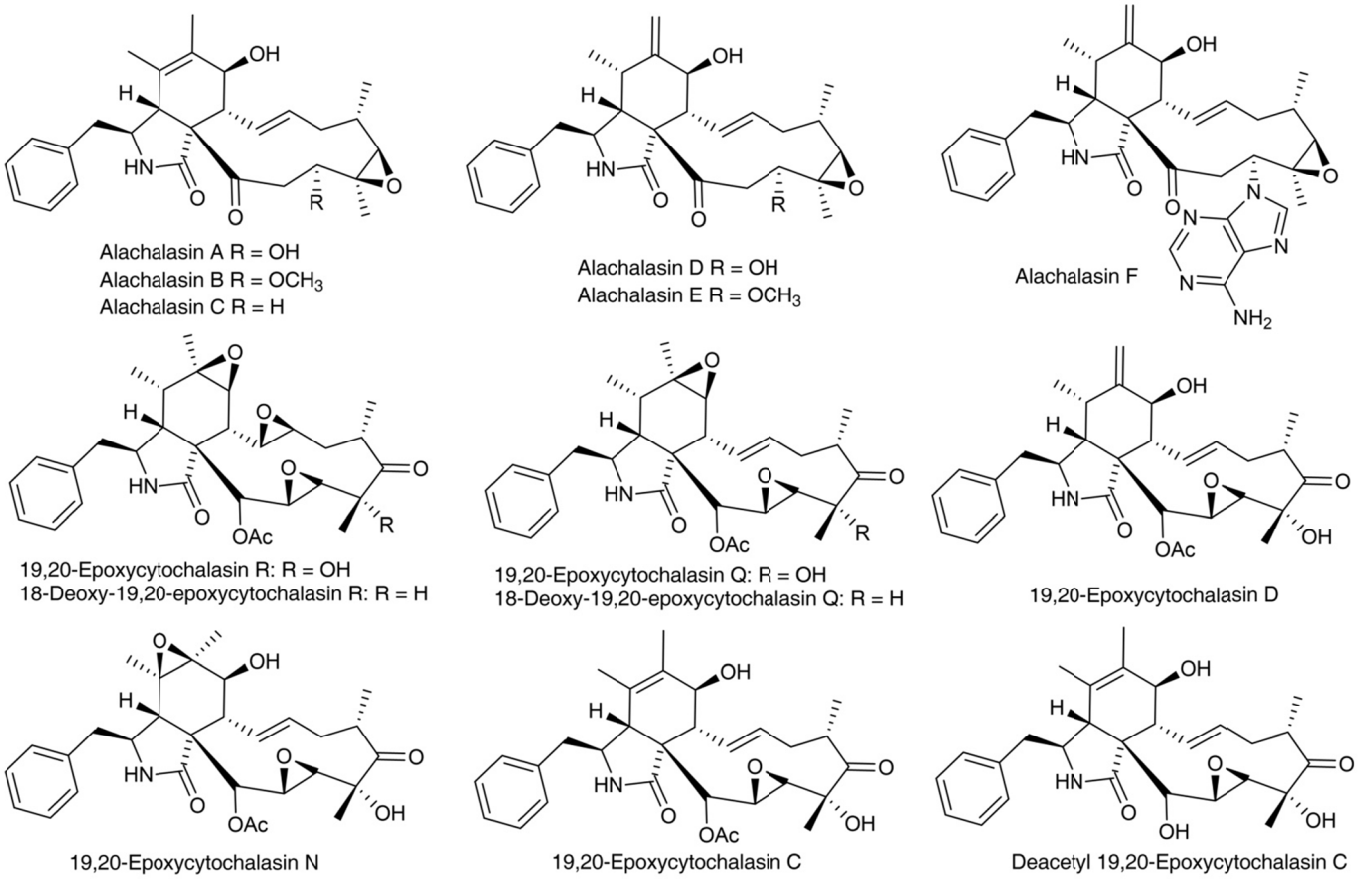

Supplementary Figure 3. Examples of C21 ketone-containing cytochalasins and their reduced derivatives[19, 20, 22-25]

(a)

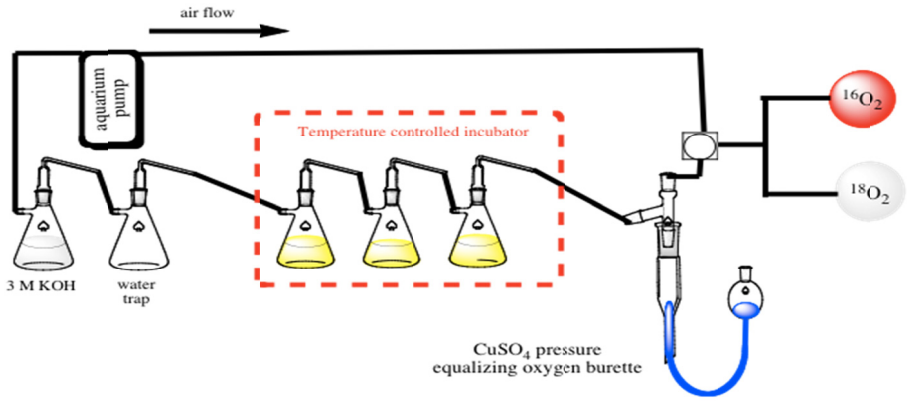

(b)

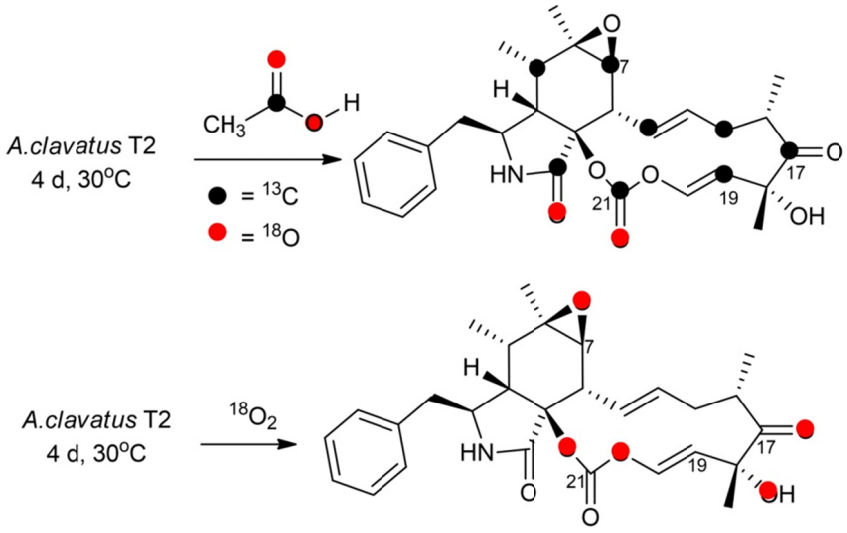

Supplementary Figure 4. Labelling study showed the origin of O and C in cytochalasin E (**1**). (a) Apparatus for $^{18}O_2$ gas feeding study. (b) Origin of O and C in cytochalasin E (**1**). The biosynthetic origin of the oxygen atoms in **1** was investigated by growing *A. clavatus* either in media supplemented with doubly labelled sodium [1-^{13}C, 1-$^{18}O_2$]acetate; or in a closed system in which consumed oxygen is replaced by $^{18}O_2$. Labelled **1** was purified from both fermentation media followed by ^{1}H and ^{13}C NMR characterization. A slight upfield shift ($\Delta\delta_c \sim 0.05$ ppm) for ^{13}C connected to ^{18}O is used as an indicator of the source of oxygen atoms in **1** (see **Supplementary Fig. 5**) [26, 27]. Both C1 and C21 of **1** recovered from culture supplemented with doubly labelled acetate displayed this characteristic shift, consistent with the hypothesis that these carbonyl oxygen atoms are derived from acetate during polyketide backbone assembly. In contrast, the signals of C6, C7, C9, C17, C18, C20, and C21 in **1** recovered from the $^{18}O_2$ experiment all exhibited this upfield shift. The C17 shift (δ_C 211.752 ppm to 211.702 ppm) indicates the C17 ketone is introduced after completion of the PKS-NRPS assembly line. The shift observed for C9 (δ_C 87.200 ppm to 87.162 ppm), C20 (δ_C 142.084 ppm to 142.060 ppm) along with the presence of two isotope shifts for C21 (δ_C 149.297 ppm to 149.288 and 149.279 ppm), confirmed that the carbonate oxygen atoms are derived from molecular oxygen, thereby pointing to an insertion pathway catalysed by an oxygenase.

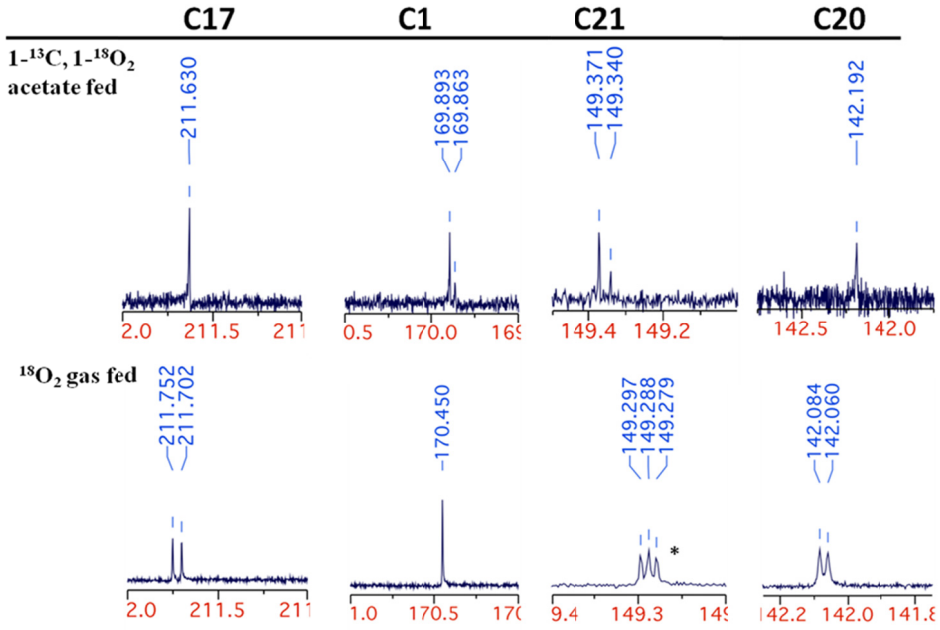

* Presence of two isotope shifts is due to incorporation of one and two ^{18}O atoms into the carbonate moiety.

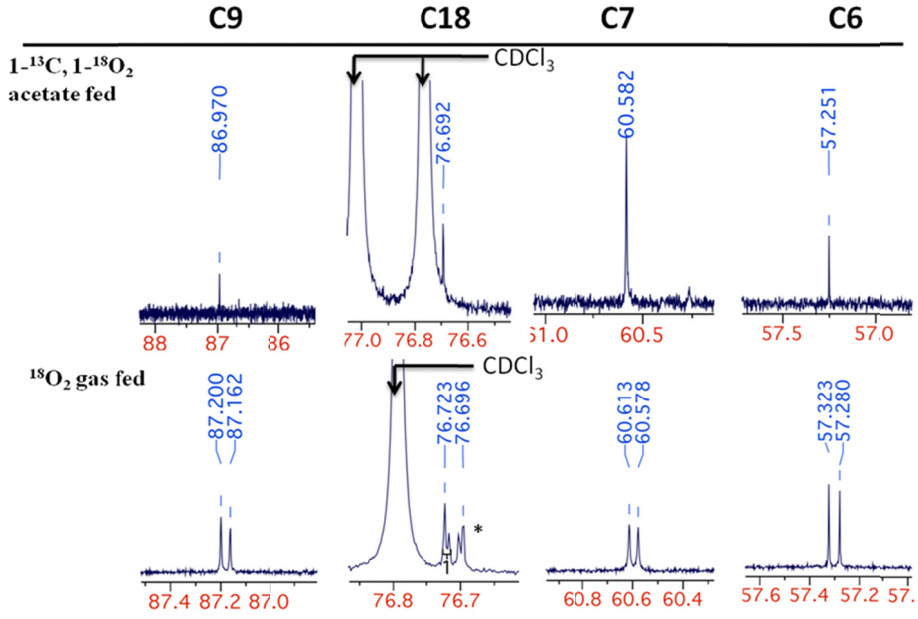

* Presence of smaller shifts (~0.005 ppm) are due to the β-isotope shift of ^{18}O at C17.

Supplementary Figure 5. Individual peaks in ^{13}C NMR ($CDCl_3$) of labelled Cytochalasin E isolated from the study shown in Supplementary Fig. 4.

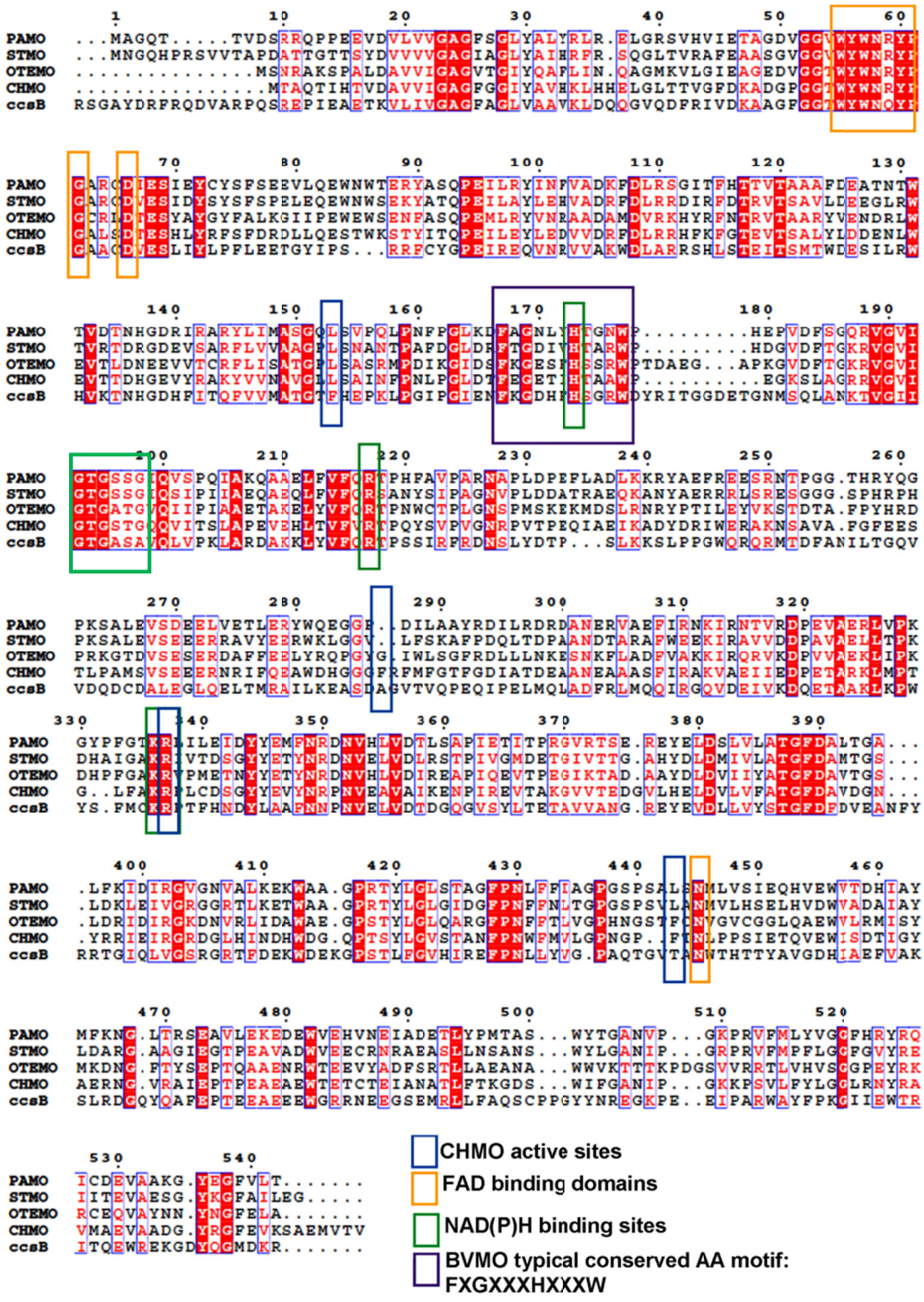

Supplementary Figure 6. Sequence alignment of representative Baeyer-Villiger monooxygenases. Highly conserved sequences for type I BVMO are found in CcsB, including the fingerprint motif FXGXXXHXXXW that is important for domain movement and NADPH binding, as well as the strictly conserved active site arginine (Arg-421) that stabilizes the Fl-4a-OO- anion through electrostatic interactions. PAMO: phenylacetone monooxygenase; STMO: Steroid monooxygenase; OTEMO: 2-oxo-Δ^3-4,5,5- Trimethylcyclopentenylacetyl-CoenzymeA monooxygenase; CHMO: cyclohexanone monooxygenase

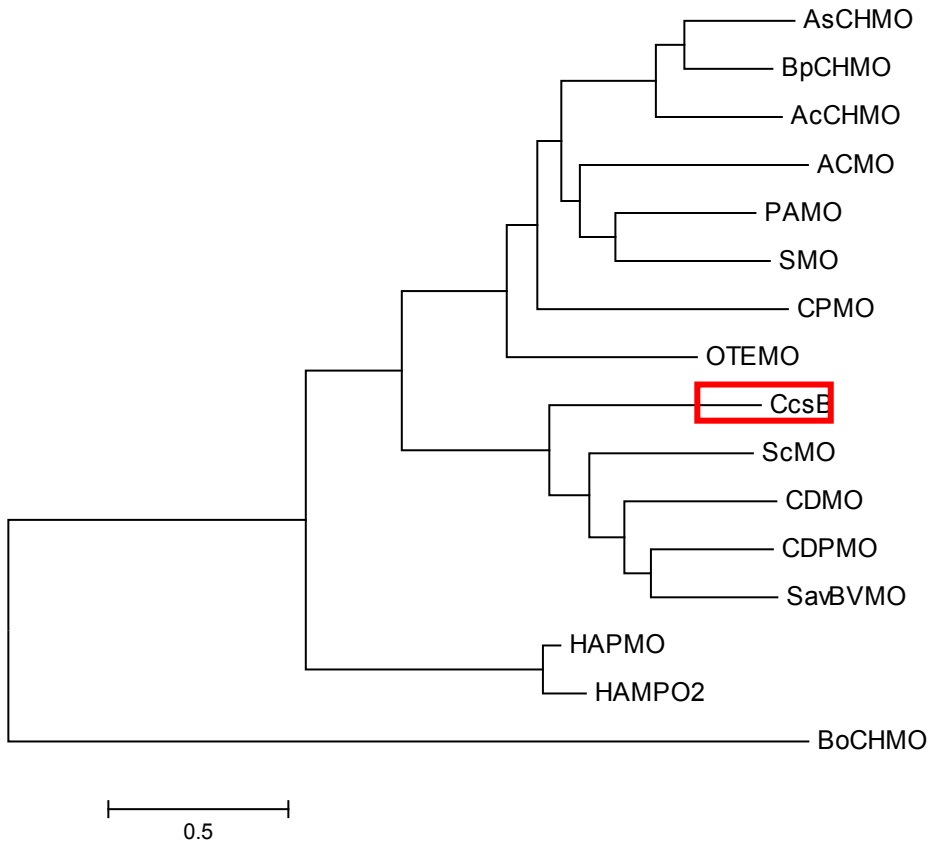

Supplementary Figure 7. Phylogenetic analysis of cloned BVMO sequences. The tree shows that CcsB groups most closely with cyclododecanone monooxygenase (CDMO) and cyclopentadecanone monooxygenase (CPDMO), thereby inferring CcsB may catalyze a BV modification on a ketone site within a macrocycle. The BVMOs are listed with their species as follows: AsCHMO: cyclohexanone monooxygenase from *Arthrobacter sp.* L661, (ABQ10653.1); BpCHMO: cyclohexanone monooxygenase from *Brachymonas petroleovorans* strain CHX(AAR99068.1); AcCHMO: cyclohexanone monooxygenase from *Acinetobacter sp.* strain NCIMB 9871 (BAA86293.1); ACMO: acetone monooxygenase from *Gordonia sp.* TY-5 (BAF43791.1); PAMO: phenylacetone monooxygenase from *Thermobifida fusca*strain YX (AAZ55526.1); SMO: steroid monooxygenase from *R. rhodochrous* strain IFO 3338 (AB010439.1); CPMO: cyclopentanone monooxygenase from *Comamonas sp.* strain NCIMB 9872 (BAC22652.1); OTEMO: 2-oxo-Δ^3-4,5,5-trimethylcyclopentenylacetic acid monooxygenase from *P. putida* ATCC 17453; ScMO: putative monooxygenase from *S. coelicolor* A3(2), (CAB55657.1); CDMO: cyclododecanone monooxygenase from *Rhodococcusruber* strain SC1 (AAL14233.1); CDPMO: cyclopentadecanone monooxygenase from *Pseudomonas sp.* strain HI-70 (BAE93346.1); SavBVMO: putative monooxygenase from *Streptomyces avermitilis* MA-4680 (BAC70705.1); HAPMO: 4-hydroxyacetophenone monooxygenase from *P. fluorescens* strain ACB (AAK54073.1); HAPMO2: 4-hydroxyacetophenone monooxygenase from *P. putida*JD1 (ACJ37423.1); BoCHMO: cyclohexanone monooxygenase from *Brevibacterium oxydans* IH-35A.

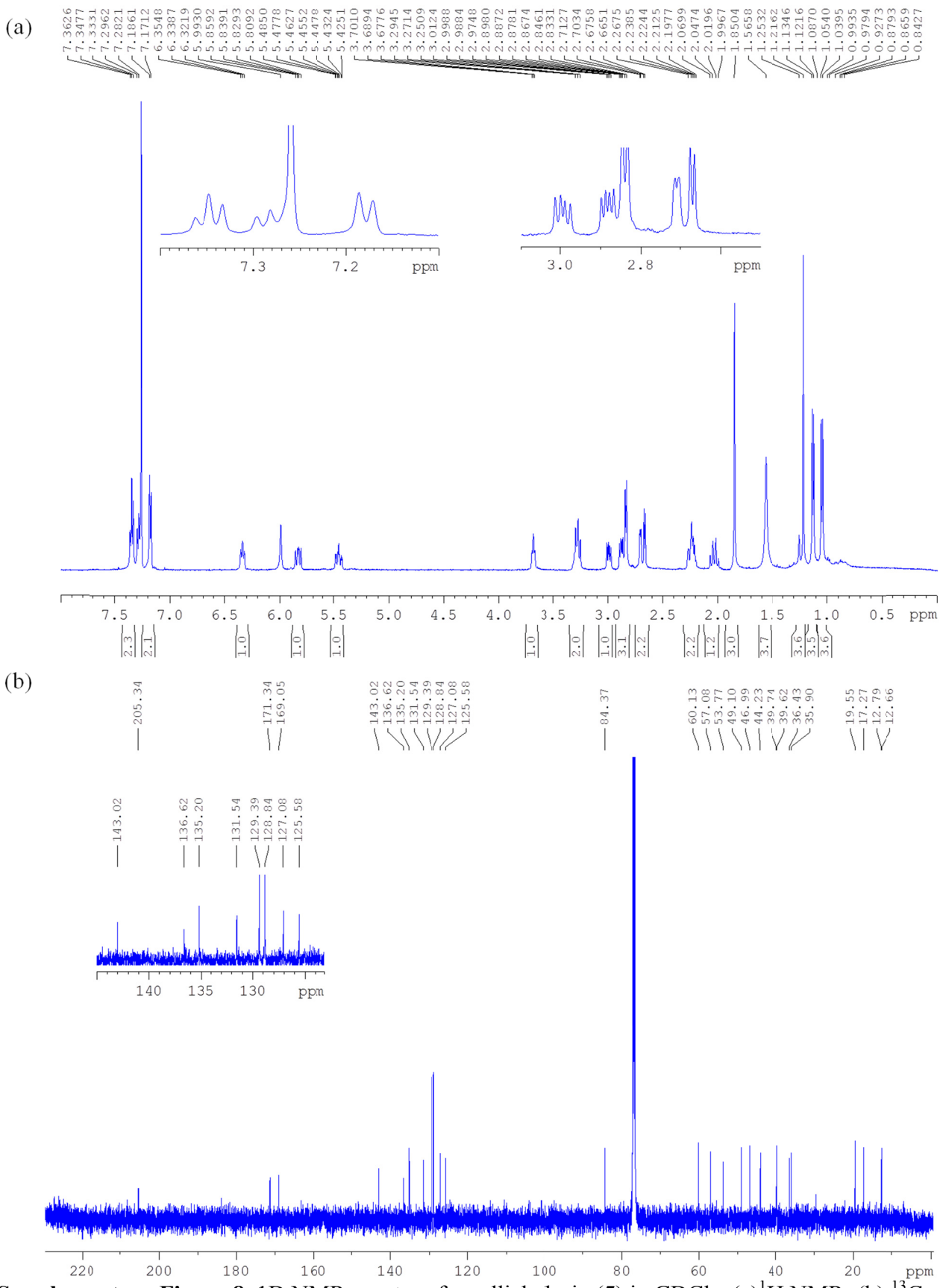

Supplementary Figure 8. 1D NMR spectra of rosellichalasin (**5**) in $CDCl_3$. (a)^{1}H NMR; (b) ^{13}C NMR

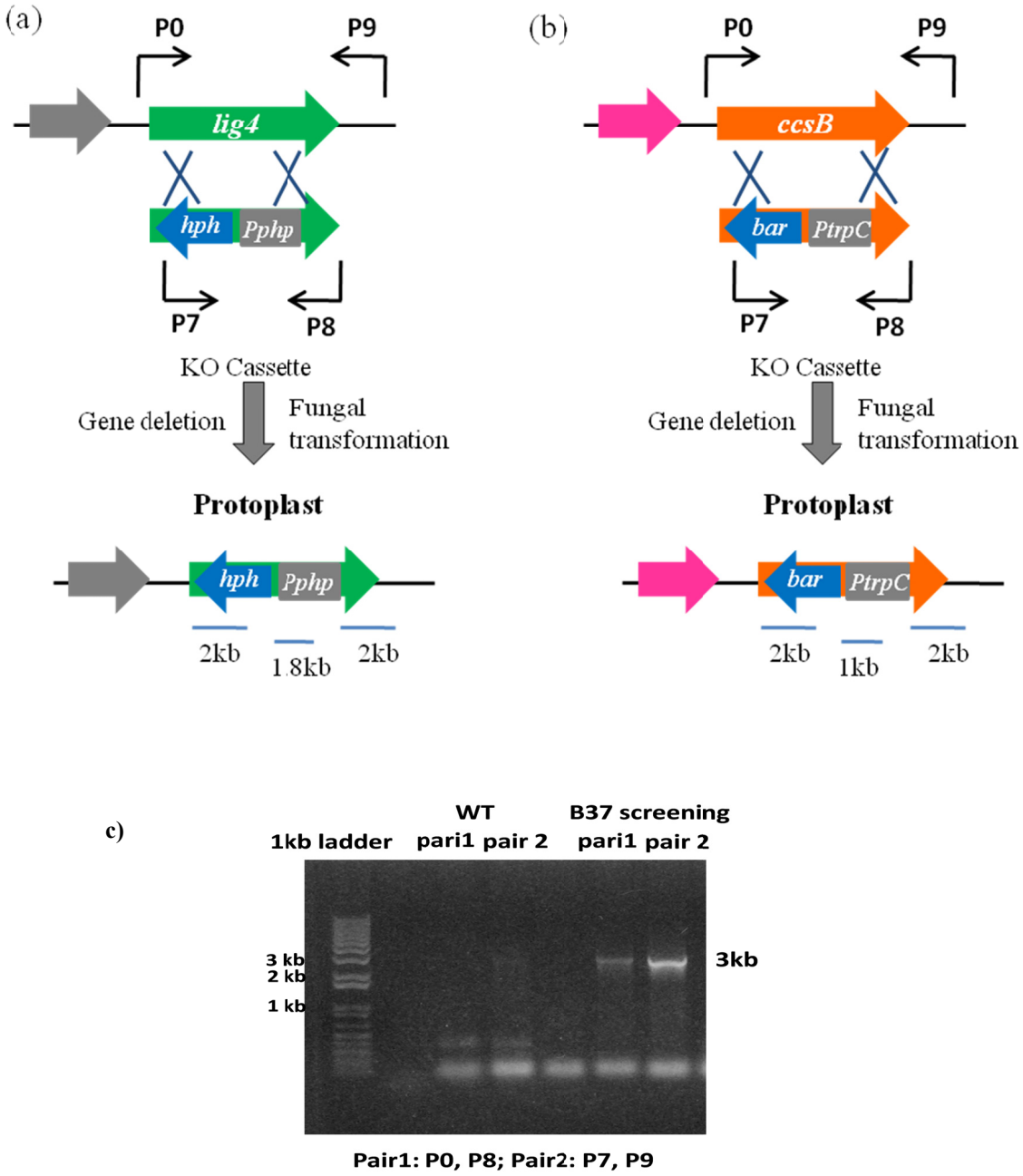

Supplementary Figure 9. Deletion of *ccsB* in *Aspergillus clavatus.* a) Gene deletion of *lig4* with *hph* (hygromycin resistance gene) cassette; b) Gene deletion of *ccsB* with *bar* cassette. c) PCR screening of *Δ ccsB*-37 mutant. Using the overproducing strain (OE::*ccsR*, *Δlig4*), the *ccsB* gene was deleted using double homologous gene replacement with the glufosinate resistance gene *bar* as a marker. Following PCR confirmation of the desired genotype one of the desired mutants (*ΔccsB*-37) was grown under stationary liquid surface culture. The culture media and mycelia were extracted with ethyl acetate, dried *in vacuo* and subjected to LC-MS analysis.

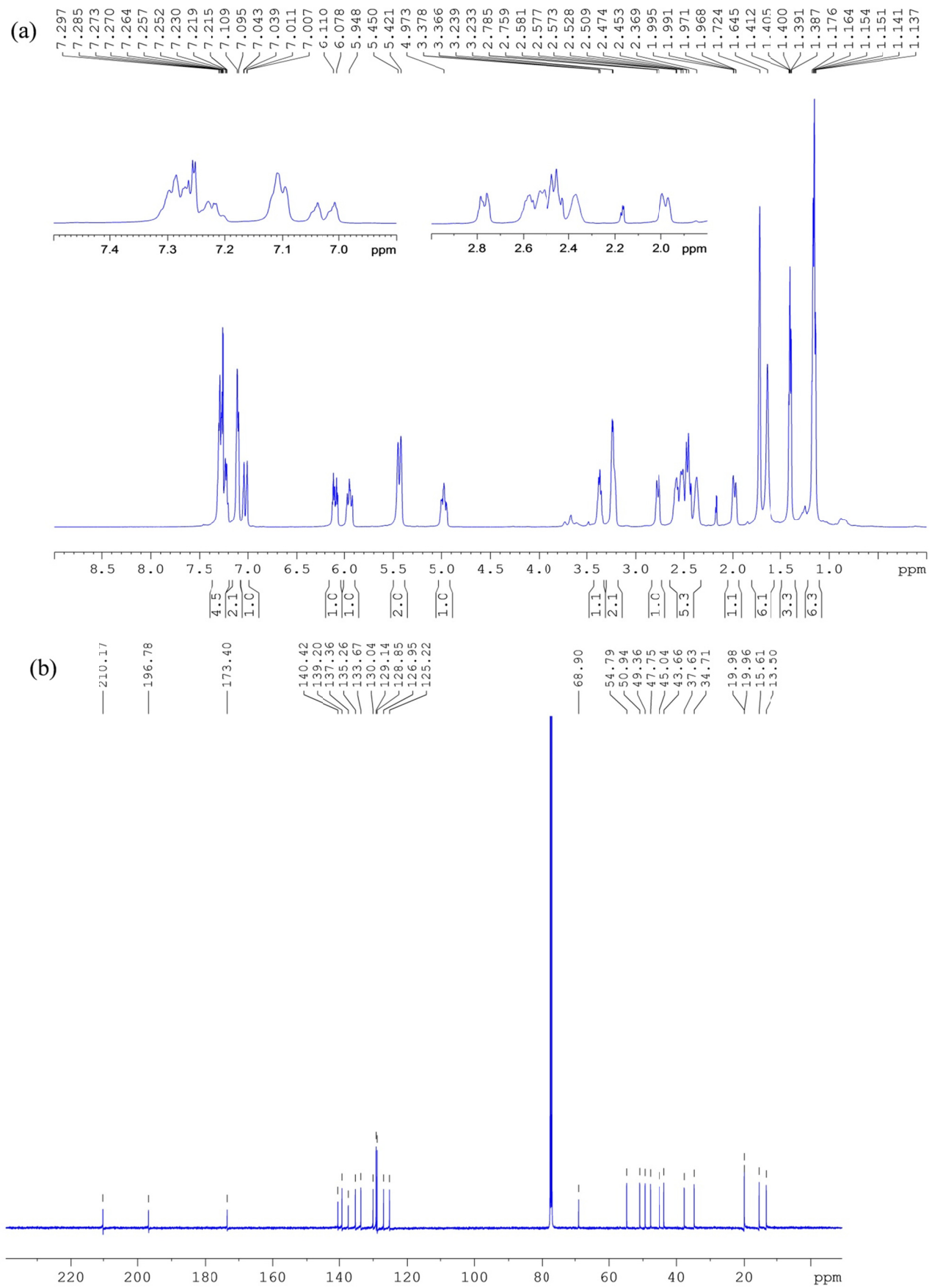

Supplementary Figure 10. 1D NMR of ketocytochalasin **7** in $CDCl_3$. (a) ^{1}H NMR; (b) ^{13}C NMR

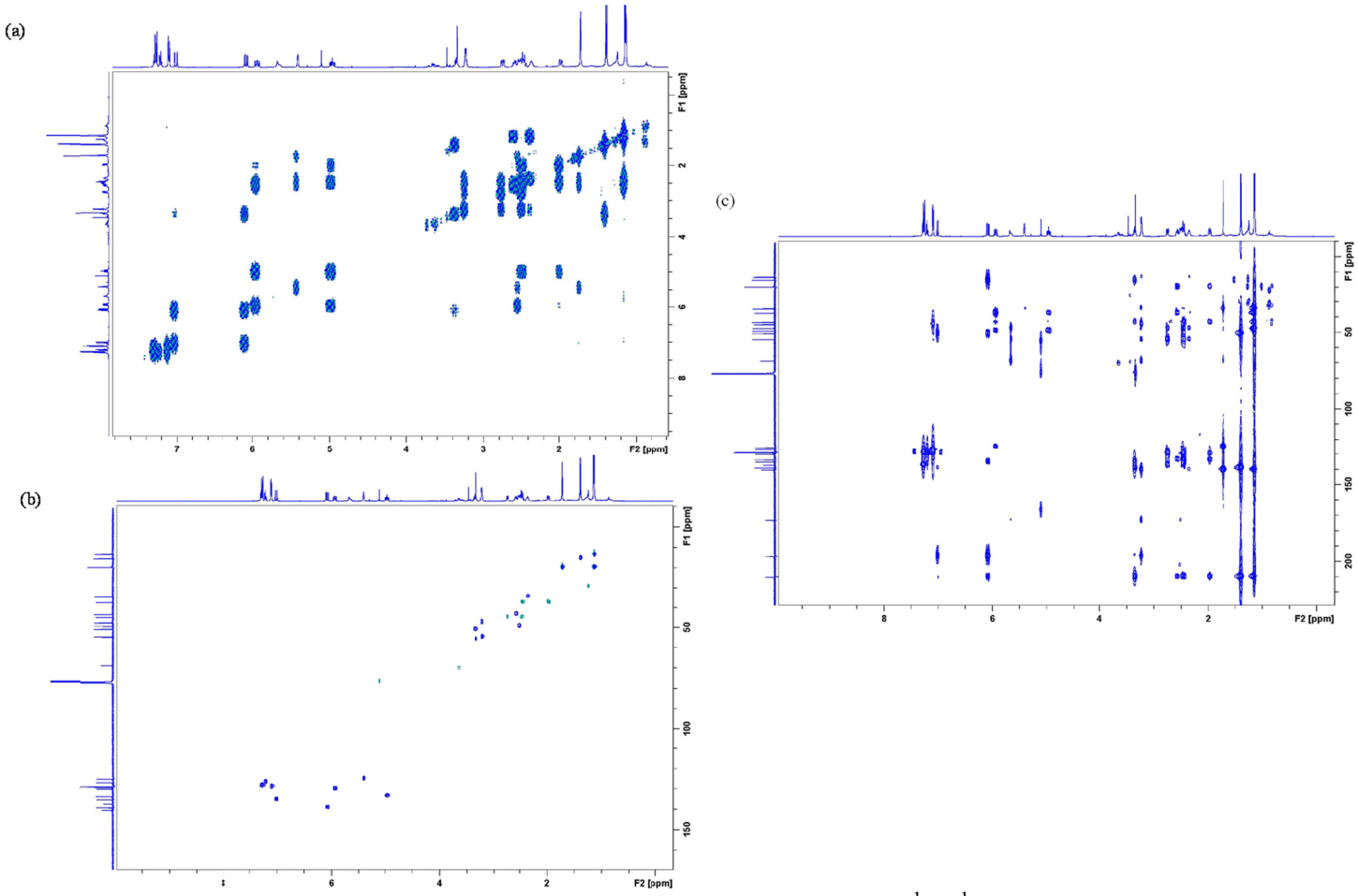

Supplementary Figure 11. 2D NMR spectra of **7** in $CDCl_3$. (a): ^1H, ^1H-COSY spectrum; (b): HSQC spectrum; (c): HMBC spectrum.

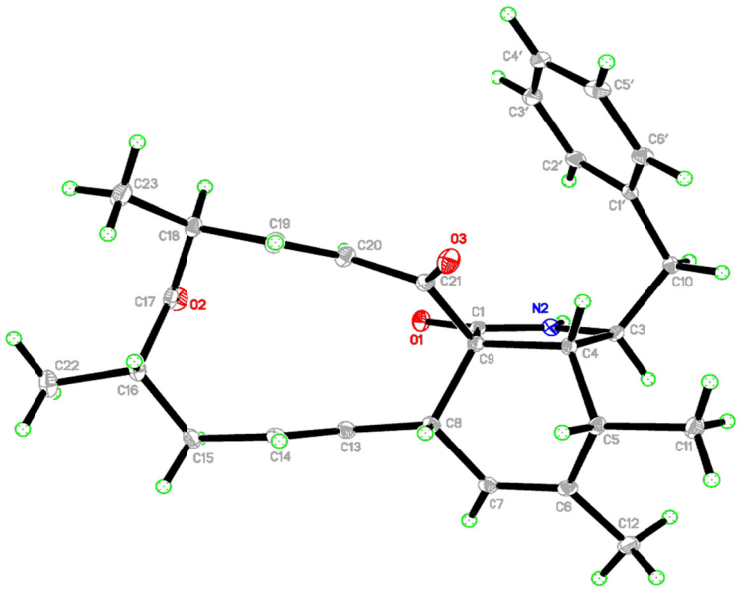

Supplementary Figure 12. ORTEP drawing of crystal structure of ketocytochalasin (**7**, CCDC 970431)

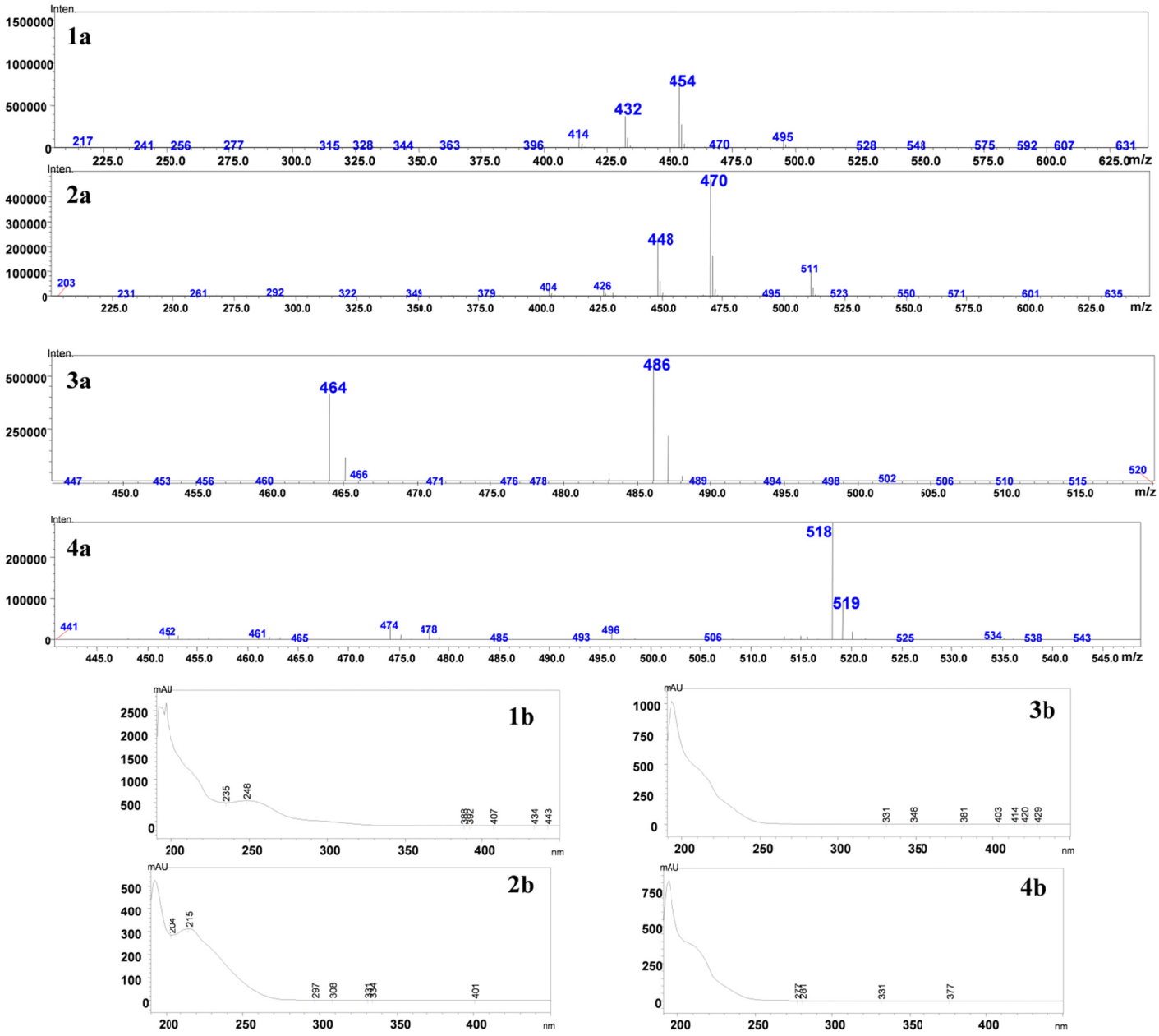

Supplementary Figure 13. UV and mass data of compounds **1**, **7-9**.
1a: MS of ketocytochalasin (**7**); 1b: UV of ketocytochalasin (**7**); 2a: MS of iso-precytochalasin (**8**); 2b: UV of iso-precytochalasin (**8**); 3a: MS of cytochalasin Z_{16} (**9**); 3b: UV of cytochalasin Z_{16} (**9**); 4a: MS of cytochalasin E (**1**); 4b: UV of cytochalasin E (**1**)

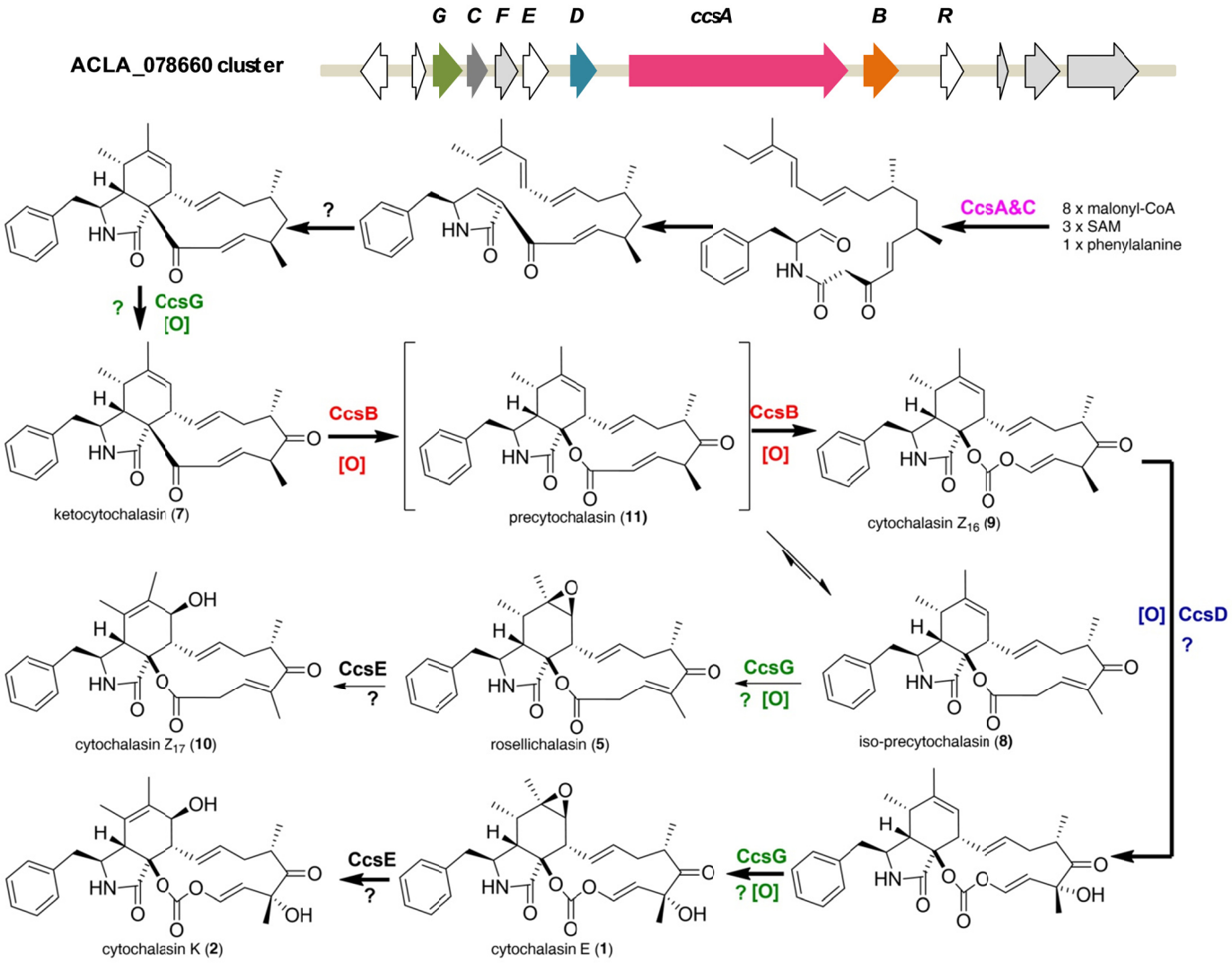

Supplementary Figure 14. Revised biosynthetic pathway for cytochalasin E (**1**) and K (**2**). Structurally, **5** and **10** represent the variations observed at C6-C7 in **1** and **2**, respectively. The simultaneous production of both **8** and **9** from the CcsB assay therefore rationalizes the co-isolation of **5** and **1** in all fungal producers

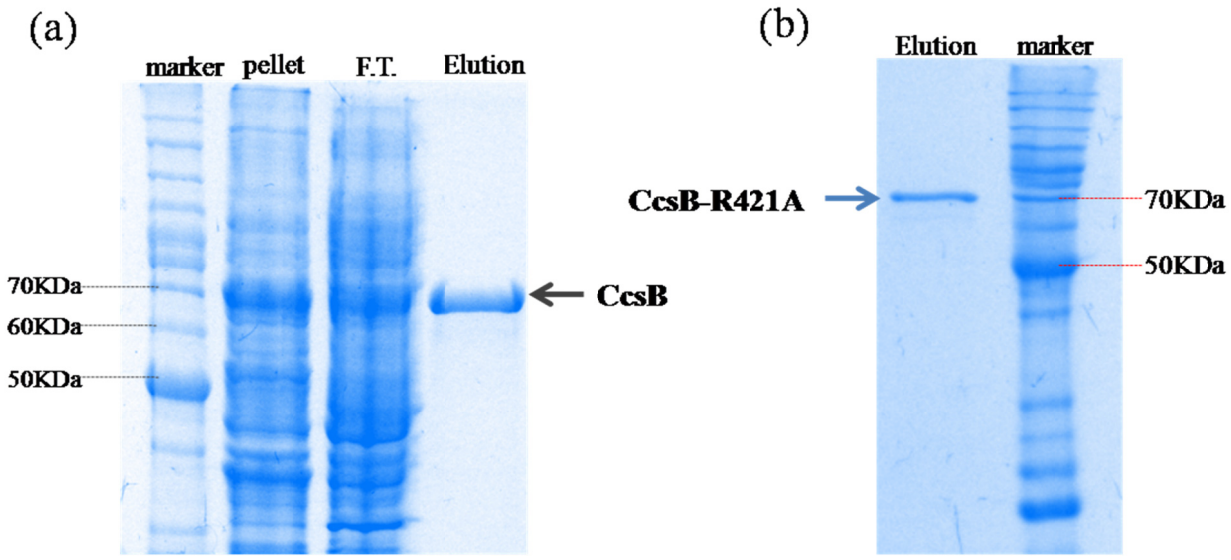

Supplementary Figure 15. Expression and purification of re-recombinant CcsB(69.5 kDa). The N-terminus of CcsB is fused to a FLAG tag, which allowed purification with anti-FLAG affinity chromatography. The first 36 residues at *N*-terminus of CcsB were removed in this construct as these were predicted to be a membrane signal peptide. (a) SDS-PAGE gel of CcsB and (b) CcsB-R421A mutant purified from *E.coli*.

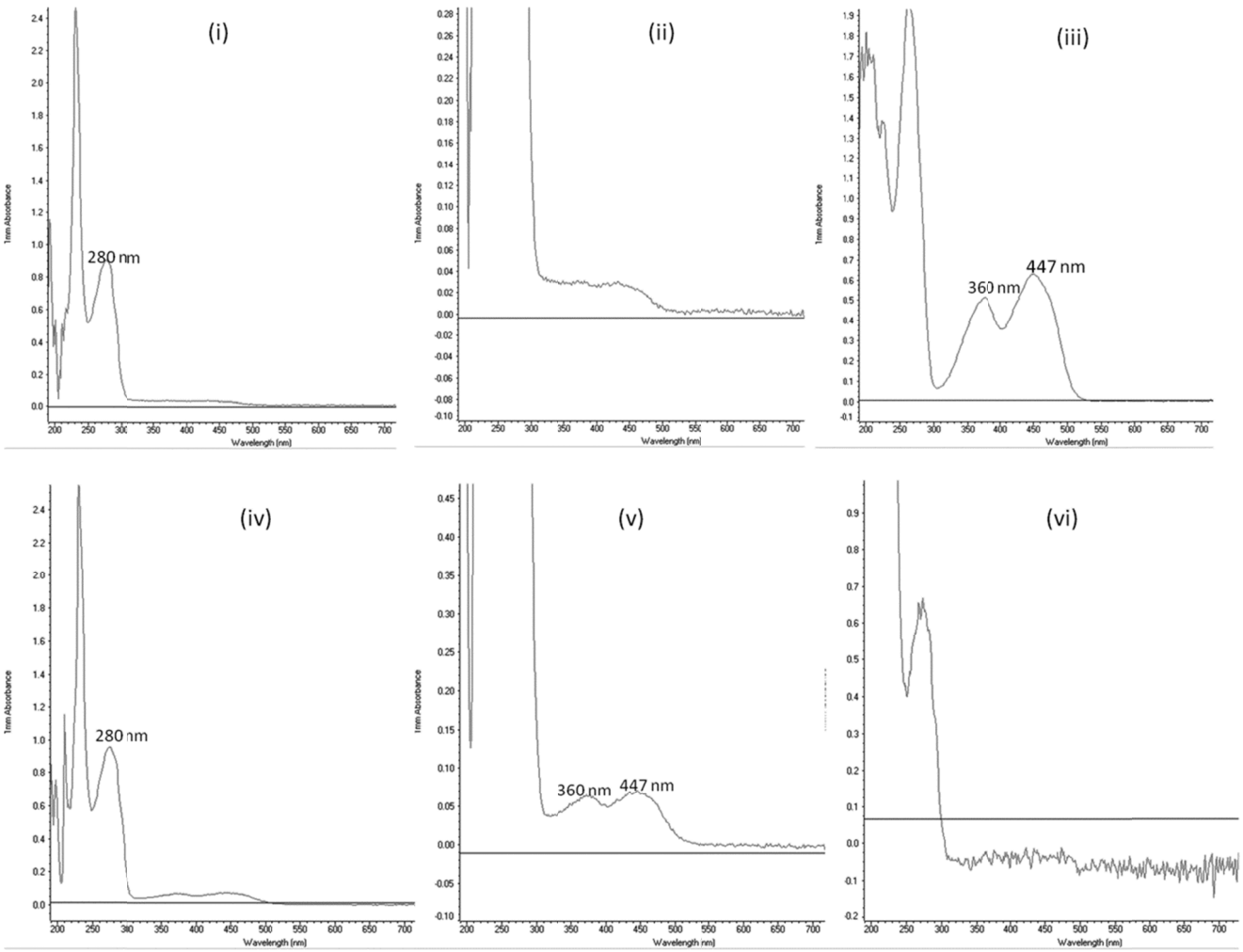

Supplementary Figure 16. Characterization of CcsB and FAD binding by UV spectra. The spectra were collected on Nanodrop 2000 UV/vis spectrophotometer. (i) UV spectrum of CcsB purified from *E. coli*; (ii) UV spectrum of CcsB purified from *E. coli* (zoomed in); For calculation of percetage of FAD binding, see **Supplementary Figure 17** in which FAD content from denatured CcsB was examined with LCMS; (iii) UV spectrum of FAD standard (0.5 mM); (iv) UV spectrum of recombinant CcsB after reconstitution with 1.2-fold excess FAD for 1 hour. Unbound FAD was removed by ultrafiltration with 30 kDa MWCO filter; (v) UV spectrum of CcsB (70 μM) after treatment with FAD (zoomed in), Based on extinction coefficient of FAD, nearly complete reconstitution of CcsB with FAD was achieved; (vi) UV specturm of CcsB sample in iv and v after treatment with NADPH and SsuE. The spectrum was collected immediately (<10 sec) after incubating 70 μM of reconstituted CcsB with 100 μM of NADPH and 10 μM SsuE.

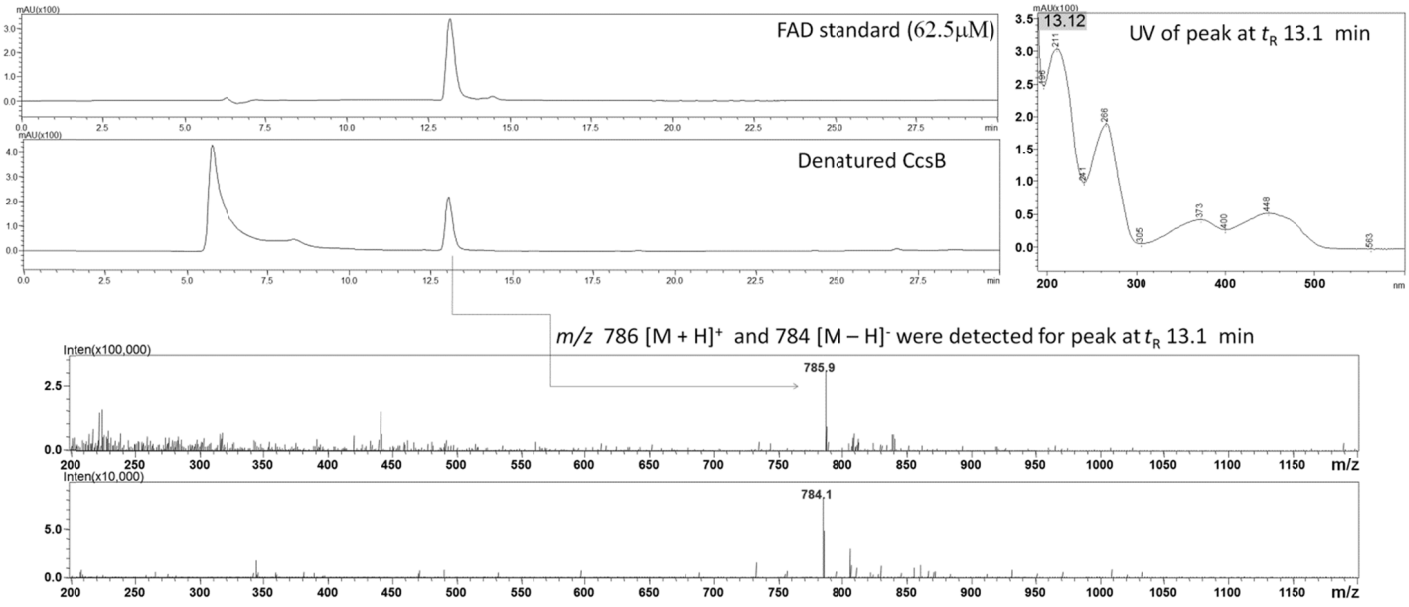

Supplementary Figure 17. Characterization of CcsB as FAD binding protein by LC-MS analysis. A standard solution of FAD was used to estalish a standard curve based on LC area at λ = 449 nm. A solution (30 μL) containing 100 μM CcsB purified from *E. coli* (**Supplementary Figure 15**) was denatured at 95°C for 10 minutes followed by centrifugation at 13,000 rpm for 2 min. The supernatant was mixed with equal volumn of MeOH and 20 μL was injected into LCMS. Using the standard curve, the amount of FAD released from denatured CcsB correspond to approximately 10% of the CcsB concentration.

a)

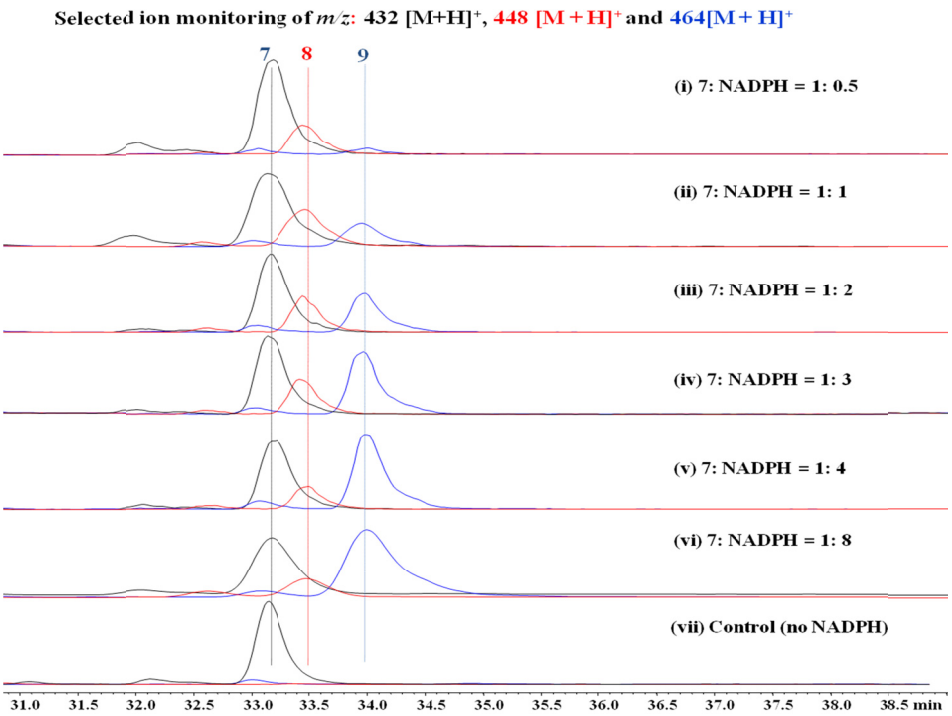

b)

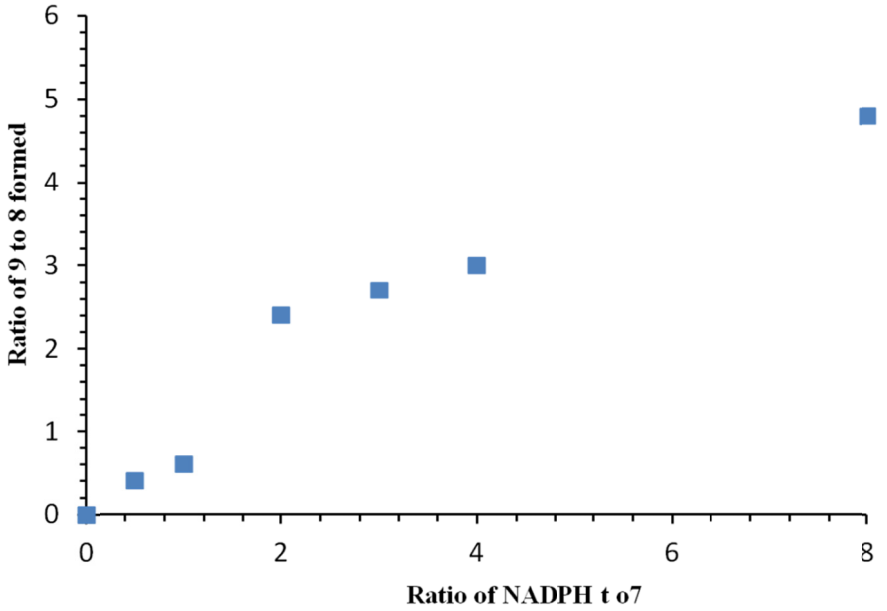

Supplementary Figure 18. Effect of NADPH concentration on product distribution. In all assays, the reaction conditions are 50 mM potassium phosphate buffer (pH 7.0), 0~3.2 mM NADPH, 20 µM FAD, 6 µM SsuE, 0.4 mM ketocytochalasin **7** and 10 µM CcsB. Reactions are performed at 25°C for 12 hours. (a) LC-MS analysis using ion monitoring of *m/z* 432 $[M+H]^+$ (**7**), 448 $[M + H]^+$ (**8**) and 464 $[M + H]^+$ (**9**). (b) Ratio of **9** to **8** formed in the reaction is strongly correlated to the molar ratio of NADPH to **7** in the reaction under specified conditions.

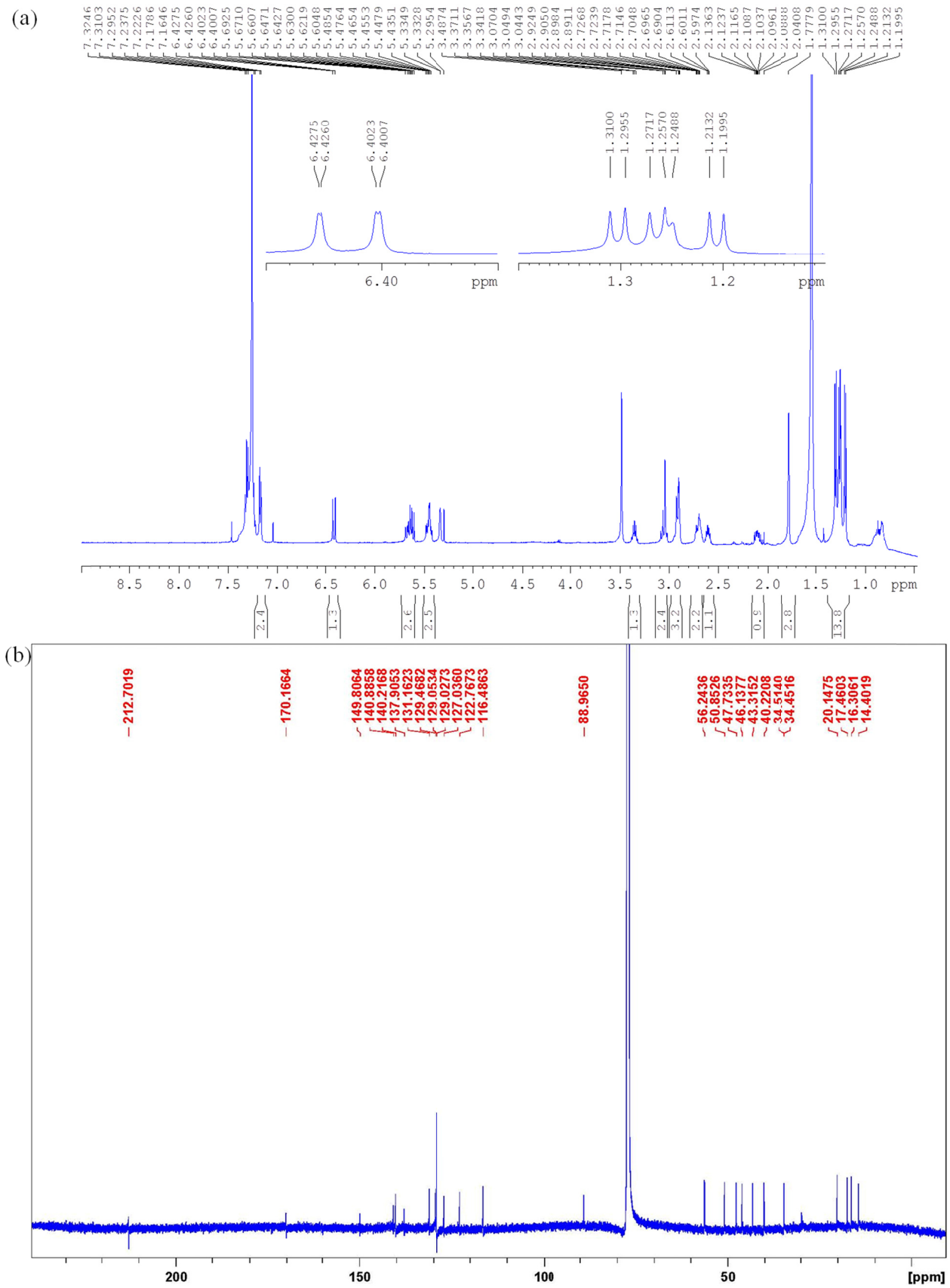

Supplementary Figure 19: 1D NMR spectra of cytochalashin Z_{16} (**9**) in $CDCl_3$.
(a). ^{1}H NMR; (b). ^{13}C NMR.

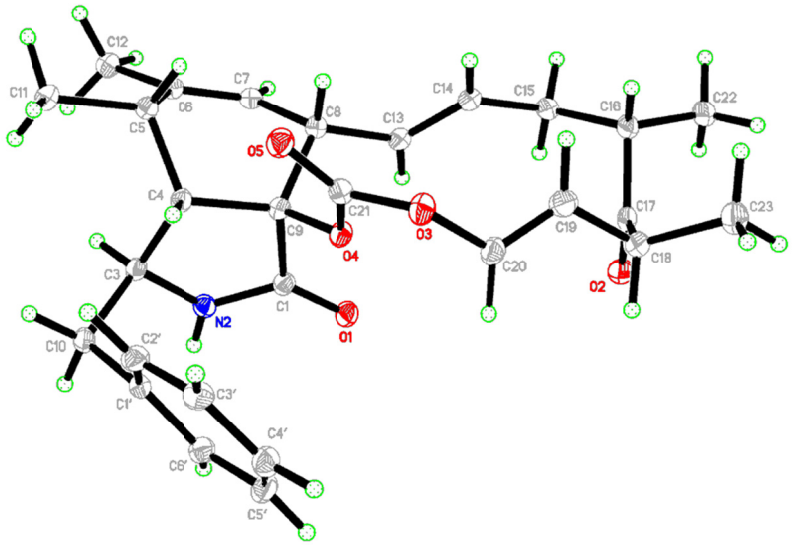

Supplementary Figure 20. ORTEP drawing of crystal structure of cytochalasin Z_{16} (**9**, CCDC 970432)

Supplementary Figure 21. Sequence alignment and verification of *ccsB* and *ccsB*-R421A mutant

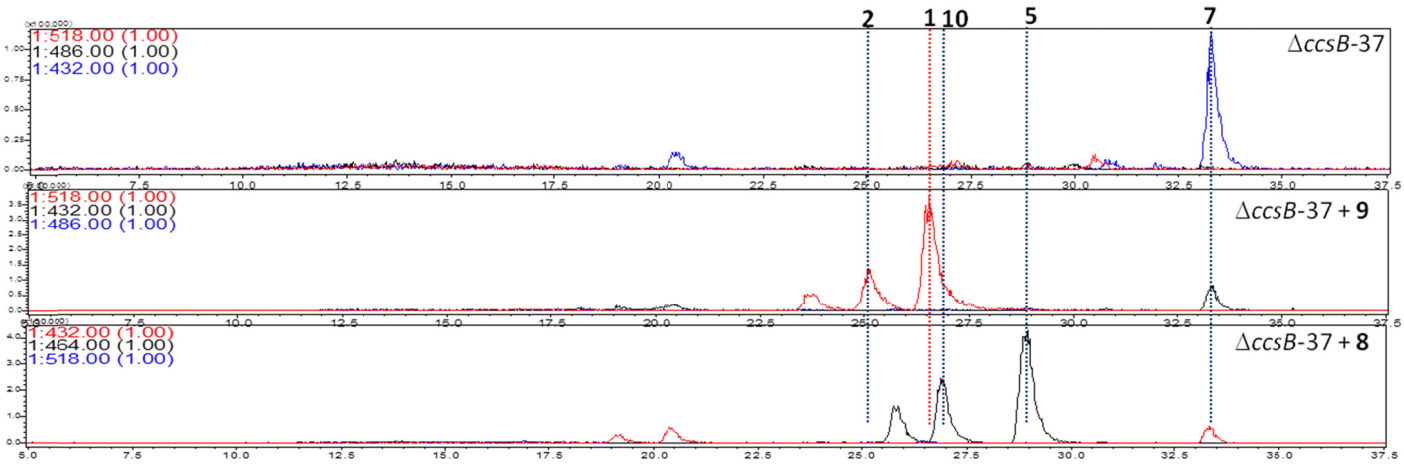

Supplementary Figure 22. LC-MS analysis of extract from the chemical complementation of **8** and **9** to *A. clavatus* Δ*ccsB*-37. The complementation results show that **9** is a precursor of **1** and **2**, while **8** is a precursor of **5** and **10**

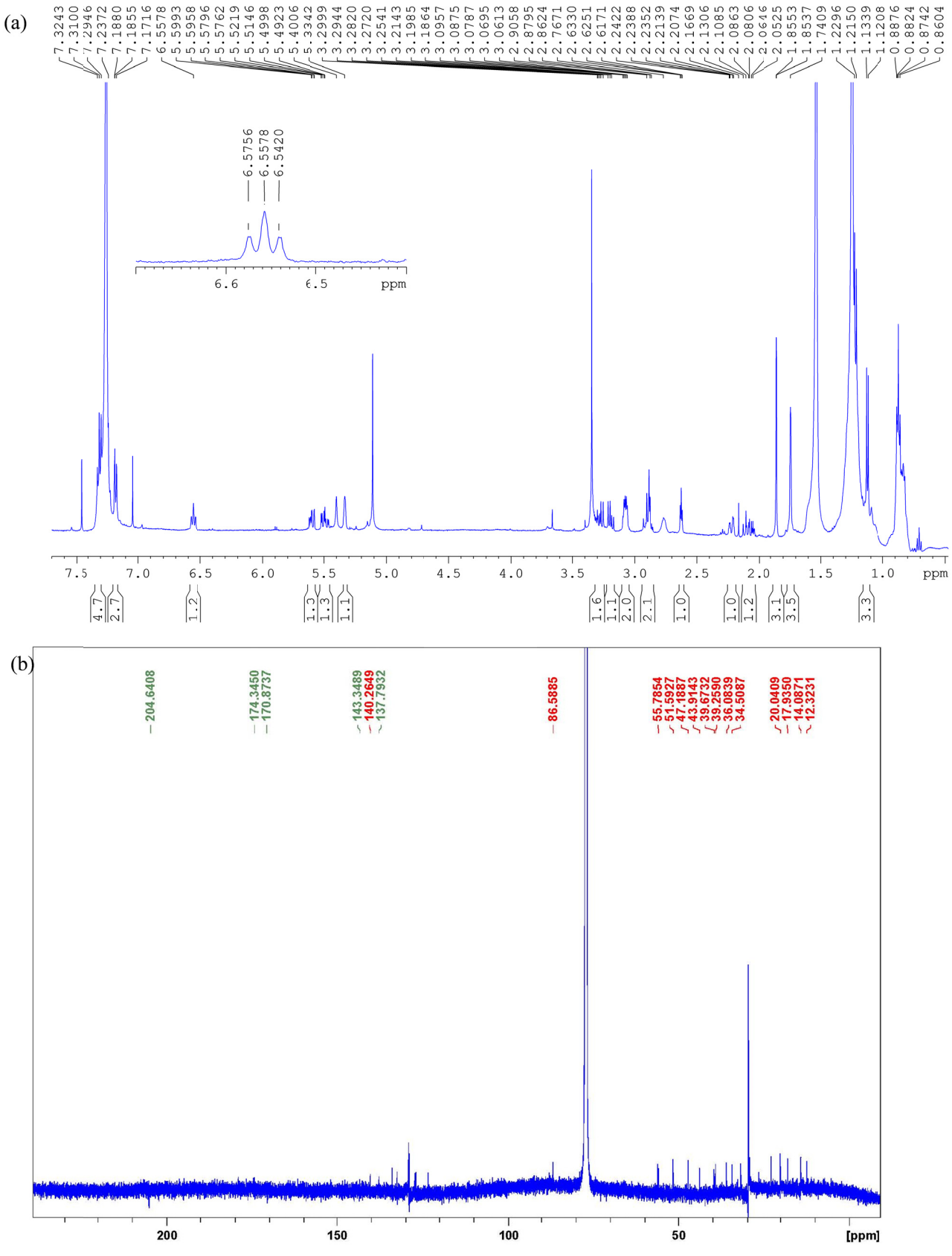

Supplementary Figure 23. 1D NMR spectra of iso-precytochalasin (**8**) in $CDCl_3$. (a) ^{1}H NMR; (b)^{13}C NMR.

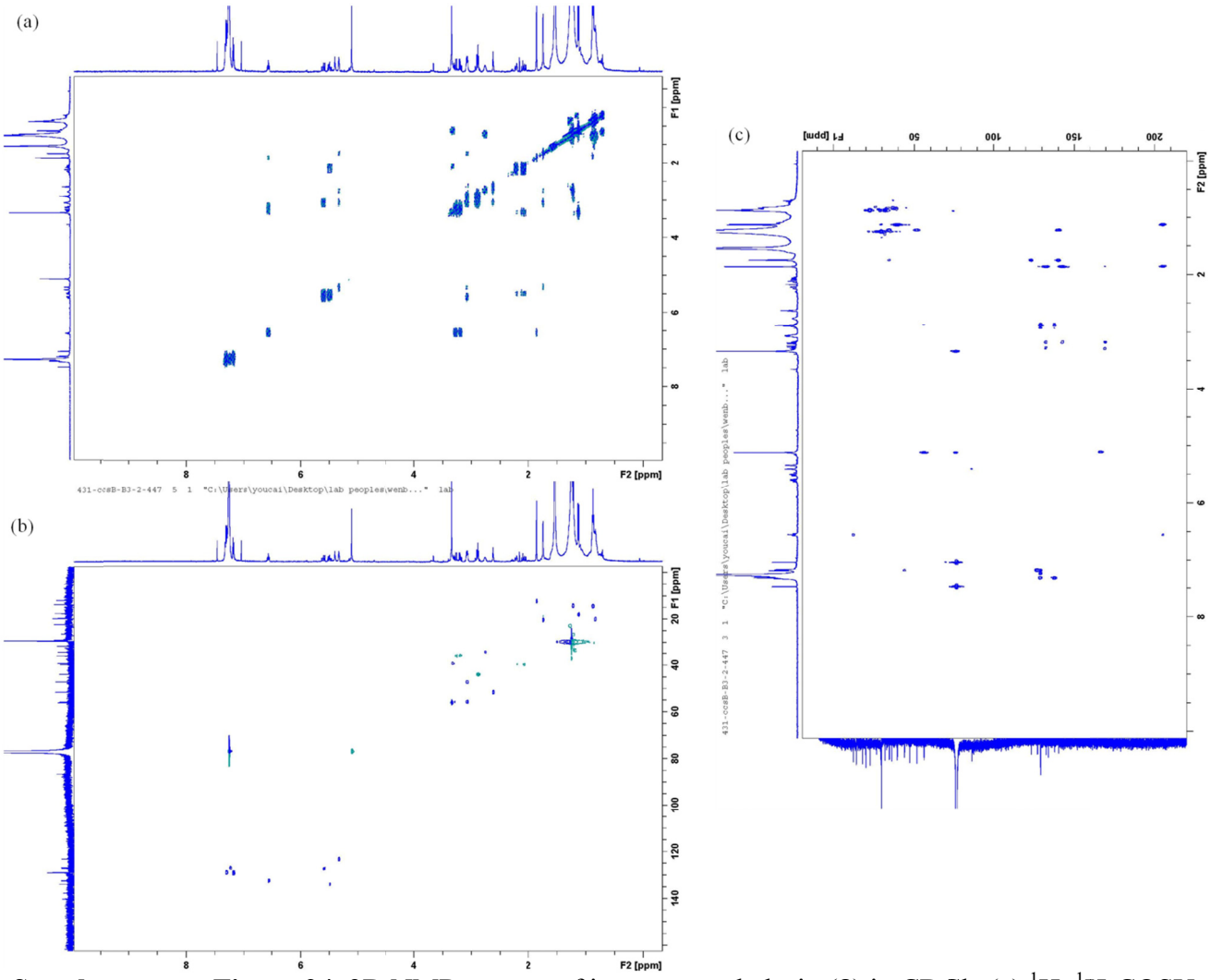

Supplementary Figure 24. 2D NMR spectra of iso-precytochalasin (**8**) in $CDCl_3$. (a) ^1H, ^1H-COSY spectrum; (b) HSQC spectrum; (c) HMBC spectrum

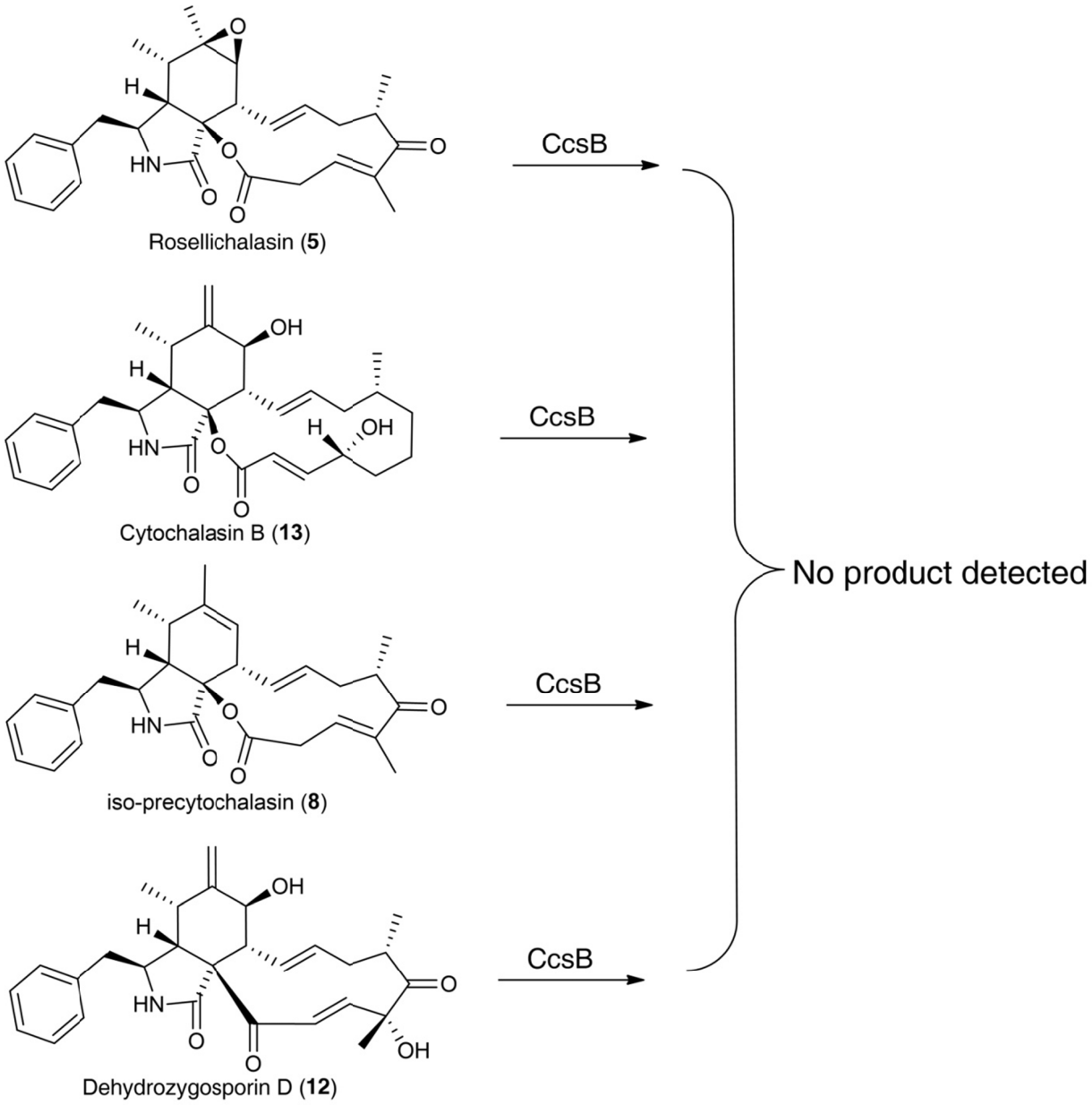

Supplementary Figure 25. *In vitro* reactions of CcsB with available cytochalasin substrates.

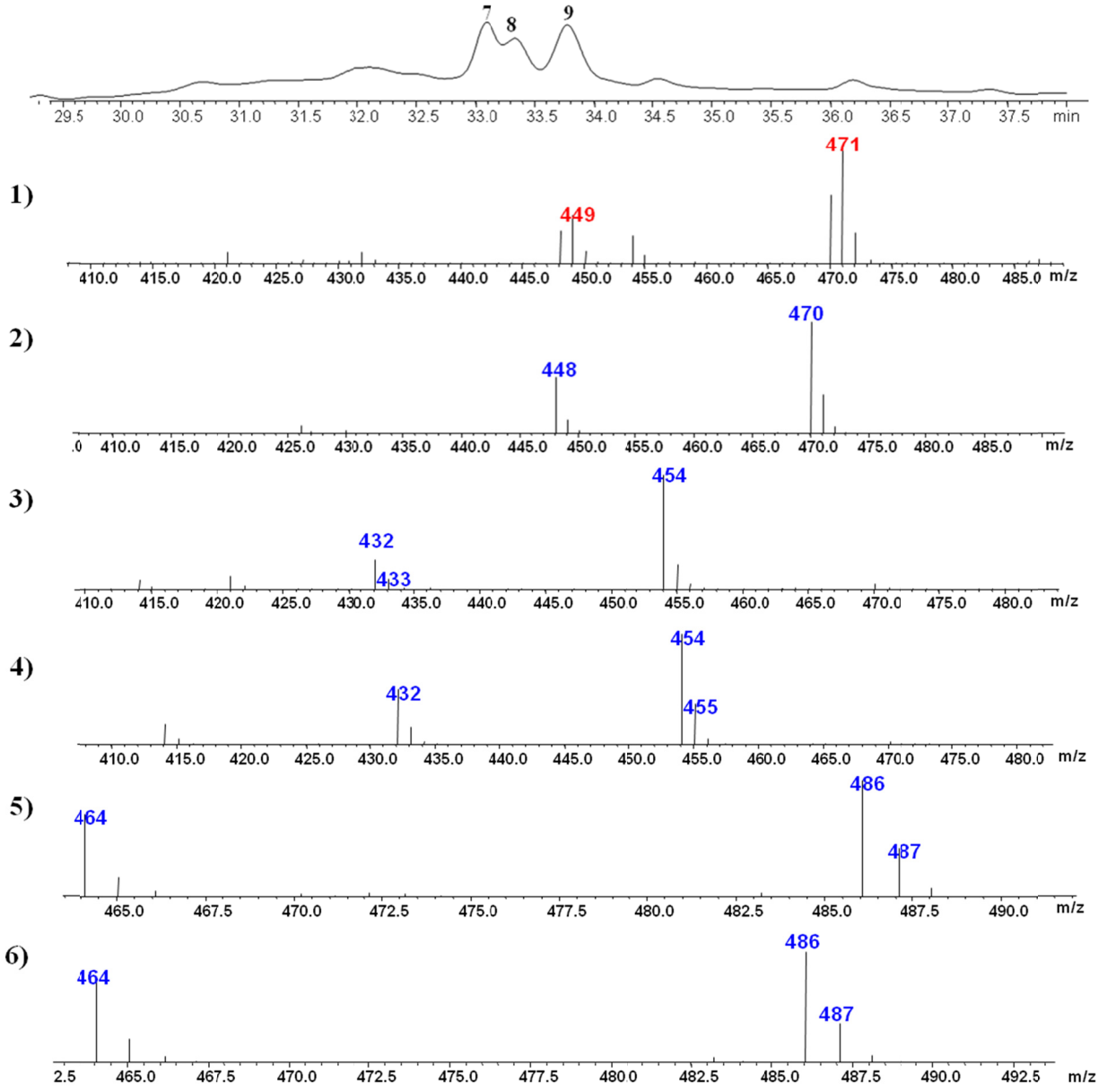

Supplementary Figure 26. In vitro assays of CcsB using buffer made in D_2O

1) MS of **8** detected in assay used buffer made in D_2O
2) MS of pure **8**
3) MS of **7** detected in assay used buffer made in D_2O
4) MS of pure **7**
5) MS of **9** detected in assay used buffer made in D_2O
6) MS of pure **9**

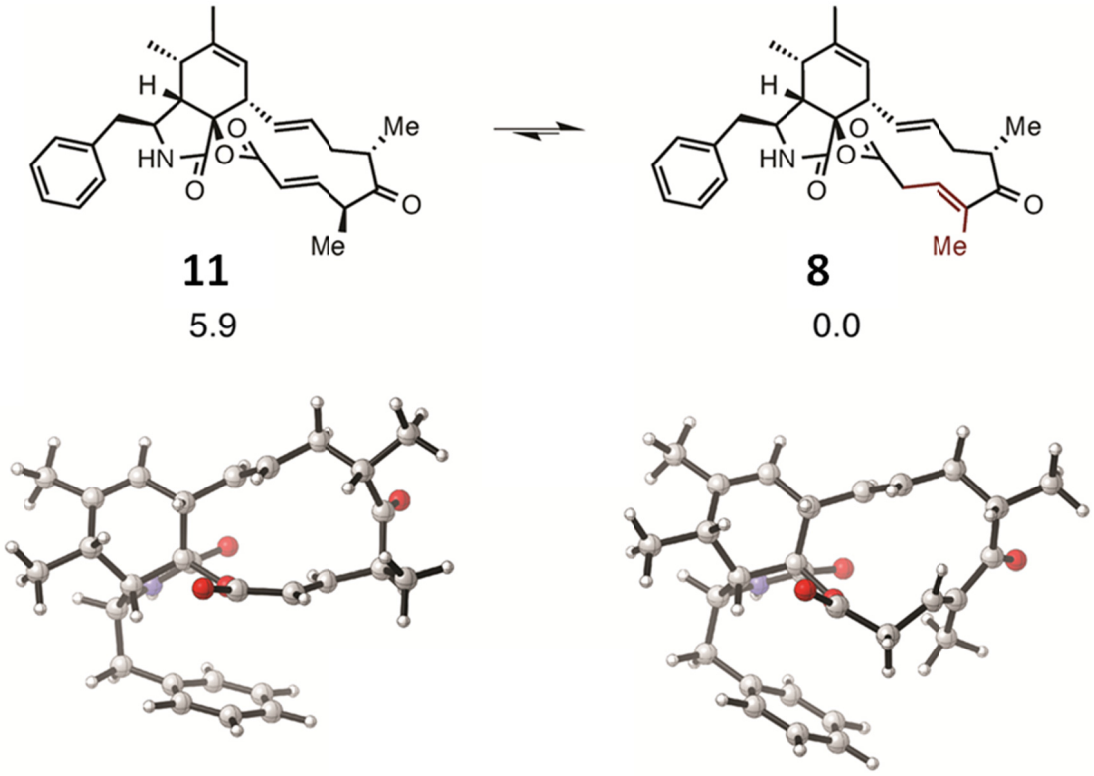

Supplementary Figure 27. QM optimized structures and relatives stabilities of intermediate **11** and **8** determined using the M06-2X/6-31+G(d,p)/SMD^{water} model chemistry. Energies reported are free energies in kcal mol^{-1} determined assuming a standard state of 1 atm and 298.15 K. The free energy of **11** is higher than that of **8** by 5.9 kcal/mol. This difference in the stabilities of these two intermediates explains why macrocycle **11** is not isolated experimentally. Intermediate **8** is likely more stable than **11** because the alkene is more substituted in intermediate **8** and also because resonance stabilization in the enone moiety of compound **8** is greater than in the unsaturated ester group of biosynthetic intermediate **11**. Differences in the ring strain may also contribute to the large difference in their stabilities. Geometries for optimization were derived from crystal structures of related cytochalasins 10-phenyl-12-cytochalasins Z_7[13] (for **11**) and 10-phenyl-[12]-cytochalasins Z_{16}[28] (for **8**).

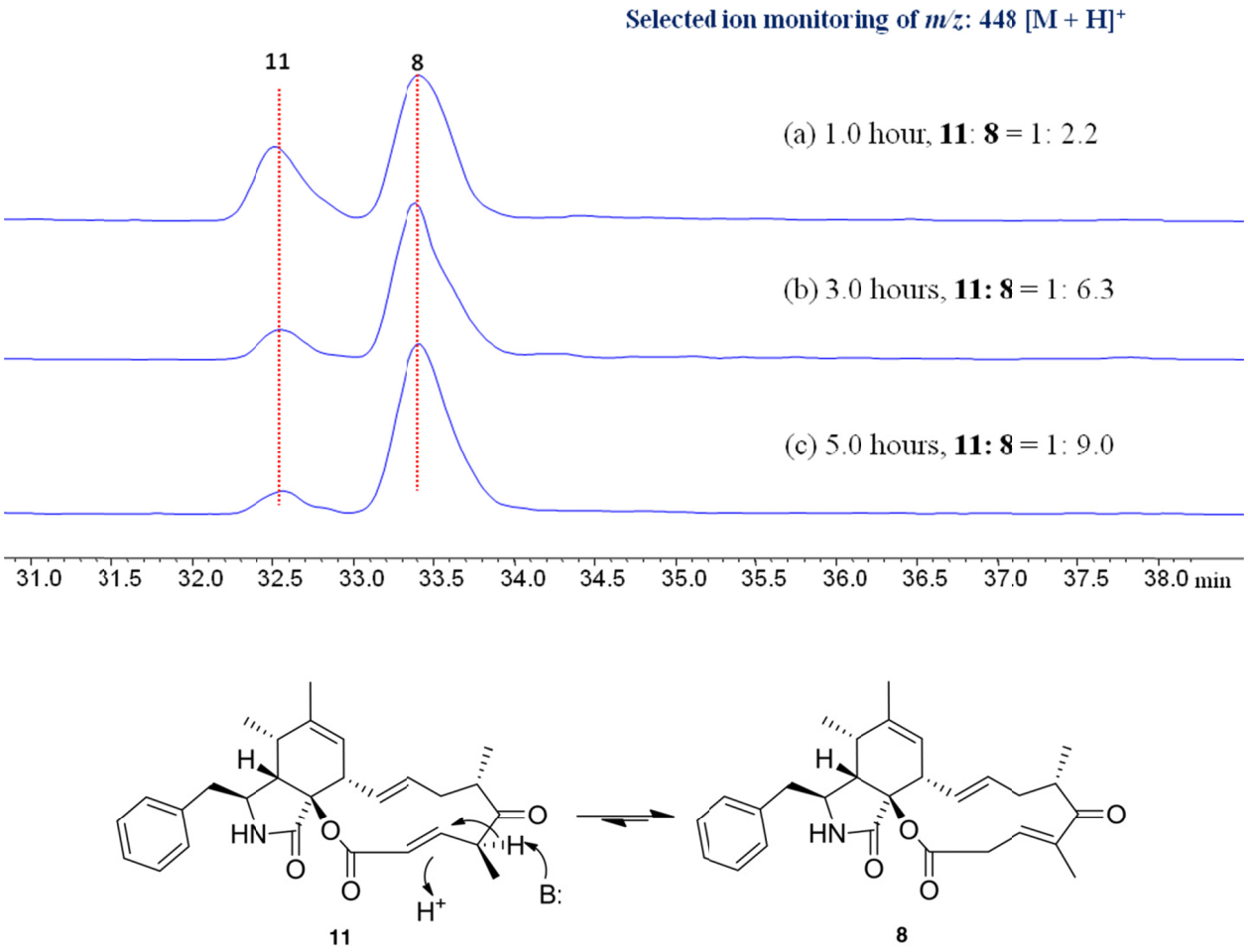

Supplementary Figure 28. A possible product of **11** deteced in the CcsB reaction. At low NADPH concentration (**9** : NADPH = 1 : 1) and early reaction time, a compound with the same *m/z* and UV as **8** can be detected in the reaction. Reaction conditions: 50 mM potassium phosphate buffer (pH 7.0), 0.4 mM NADPH, 20 μM FAD, 6 μM SsuE, 0.4 mM ketocytochalasin **9**, and 8 μM CcsB. Shown above is selected ion monitoring using *m/z* 448 $[M+H]^+$. This peak decreased at longer incubation times and is present at trace amounts. Isolation of this peak was not possible due to its instability and rapid conversion into **8** (See **Supplementary Figure 29**).

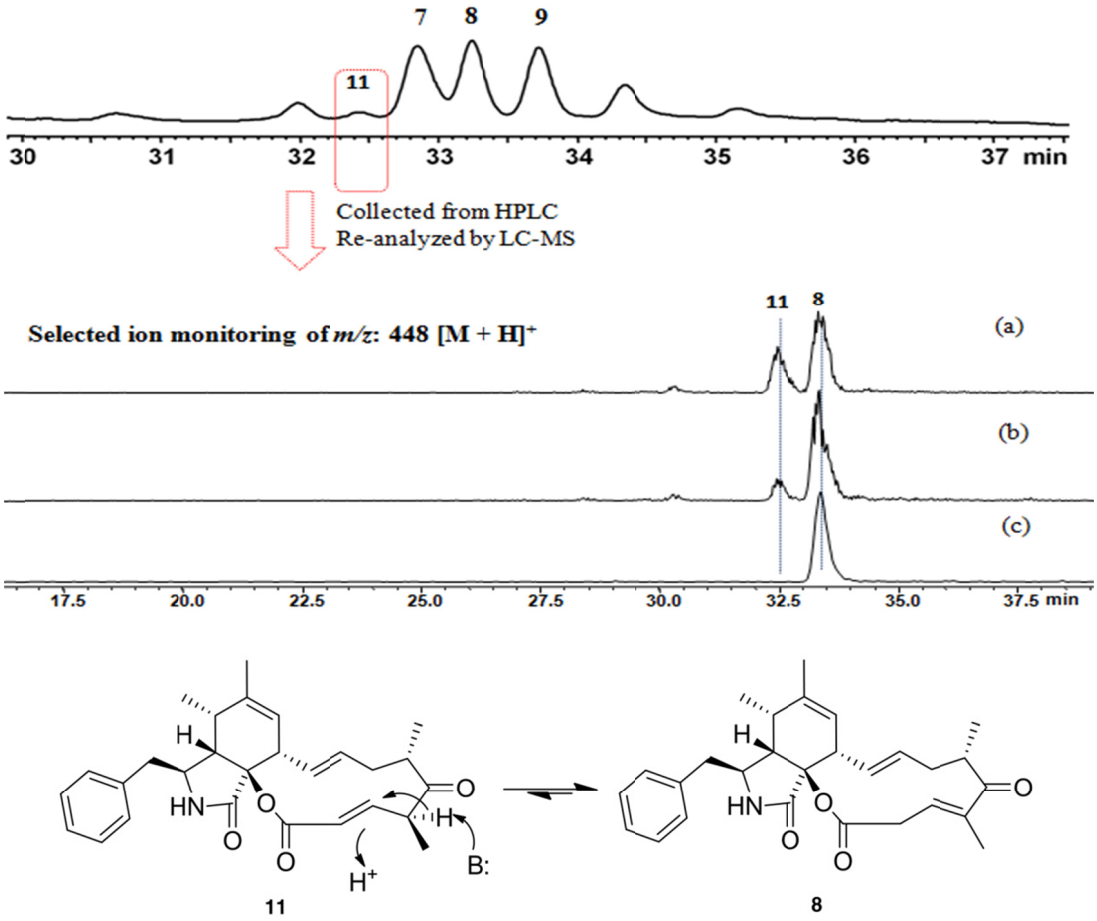

Supplementary Figure 29. Rapid isomeraization of **11** into **8** in attempt to isolate **11**. Starting with the 1 hour trace shown in here, the peak corresponding to **11** was collected during LC-MS analysis (> 90% acetonitrile in H_2O at this condition, 0.05% formic acid). The collected sample is then (a) immediately injected back into LC-MS; or (b) injected after 2 hours. (**c**) shows the authetic standard of **8**. The traces shown here are selected ion monitoring at *m/z*: 448 $[M + H]^+$. As can be seen, **11** is rapidly converted to **8**, therefore providing evidence that this peak correspond to the proposed ester intermdiate **11**. Computational calculation in **Supplementary Figure 27** supports the obervation that **8** is the dominant isomer.

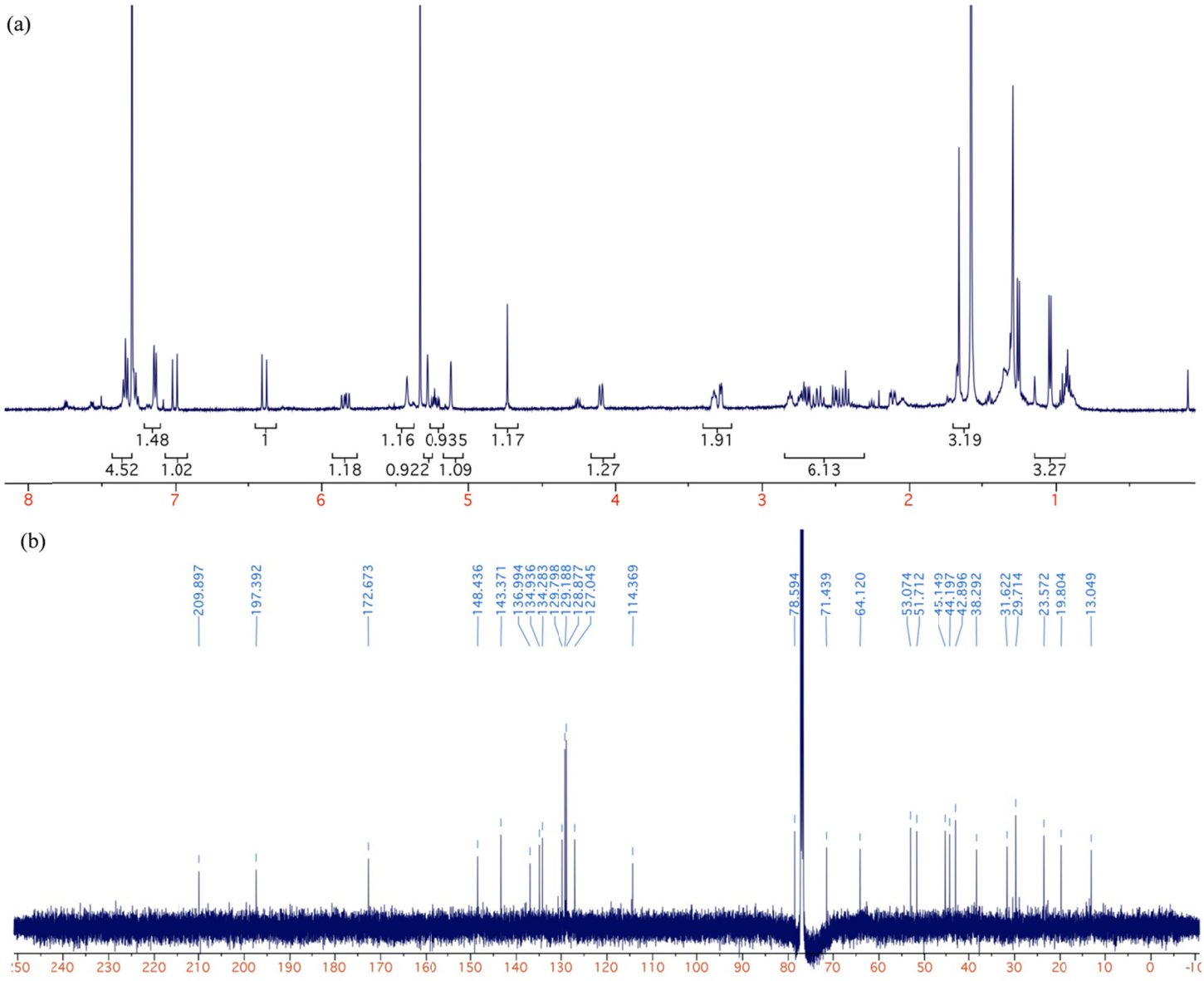

Supplementary Figure 30. 1D NMR spectra of **12** in $CDCl_3$
(a) ^{1}H NMR; (b) ^{13}C NMR

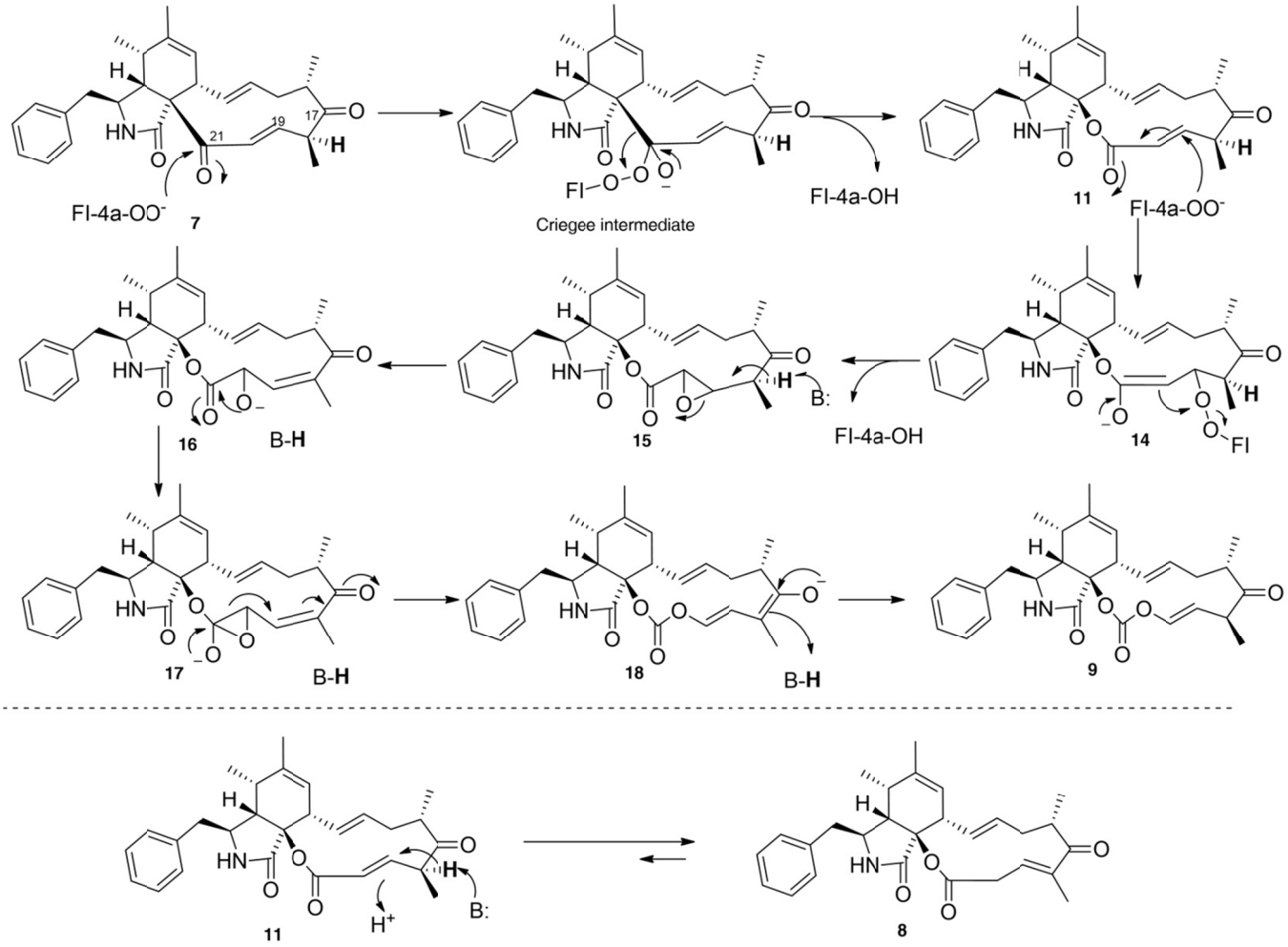

Supplementary Figure 31. Proposed reaction mechanism of CcsB in converting **7** to **8** and **9**.
The first oxygen insertion step follows that of the classic BVMO mechanism, in which attack of the Fl-4a-OO$^-$ on C21 of **7** forms the Criegee intermediate. Expected migration of tertiary C9 to the distal oxygen on Fl-4a-OO$^-$ leads to release of Fl-4a-OH and formation of ester **11**. Release of ester **11** into an aqueous environment can generate the shunt product **8**. Alternatively, **11** can remain in the active site of CcsB or be recaptured by CcsB and undergo further oxidation to yield **9**. Following reduction and regeneration of Fl-4a-OO$^-$, we propose the nucleophilic Fl-4a-OO- complex performs a 1,4-conjugate Michael addition at C19 to yield adduct **14**, which leads to the formation of epoxide **15**. Epoxidation of the α,β-unsaturated ester is observed in the cytochalasin family, such as in the epoxycytochalasin compounds.[23, 24, 29] Subsequently, base-catalysed abstraction of the acidic α-proton leads to formation of the vinylogous C17 ketone and the alcoholate anion species **16**. Attack at the neighbouring carbonyl group affords an epoxy alkoxide **17**, which can readily rearrange with aid of the distal vinylogous ketone to yield the enolate **18**. Subsequently, ketonization of C17 followed by proton abstraction from the protonated general base affords the carbonate **9**. Unlike **8**, **9** does not undergo double bond migration, possibly due to resonance stabilization through the carbonate oxygen. Examples of rearrangement of α-hydroxyl, β-diketones into esters have been reported in literature[30, 31], and can proceed under thermal or basic conditions via the proposed epoxy-tetrahedral intermediate such as shown in **17**. Furthermore, an example of Lewis-acid-promoted conversion of an α-hydroxy β-dicarbonyl compound to a carbonate rearrangement has been reported[8, 32].

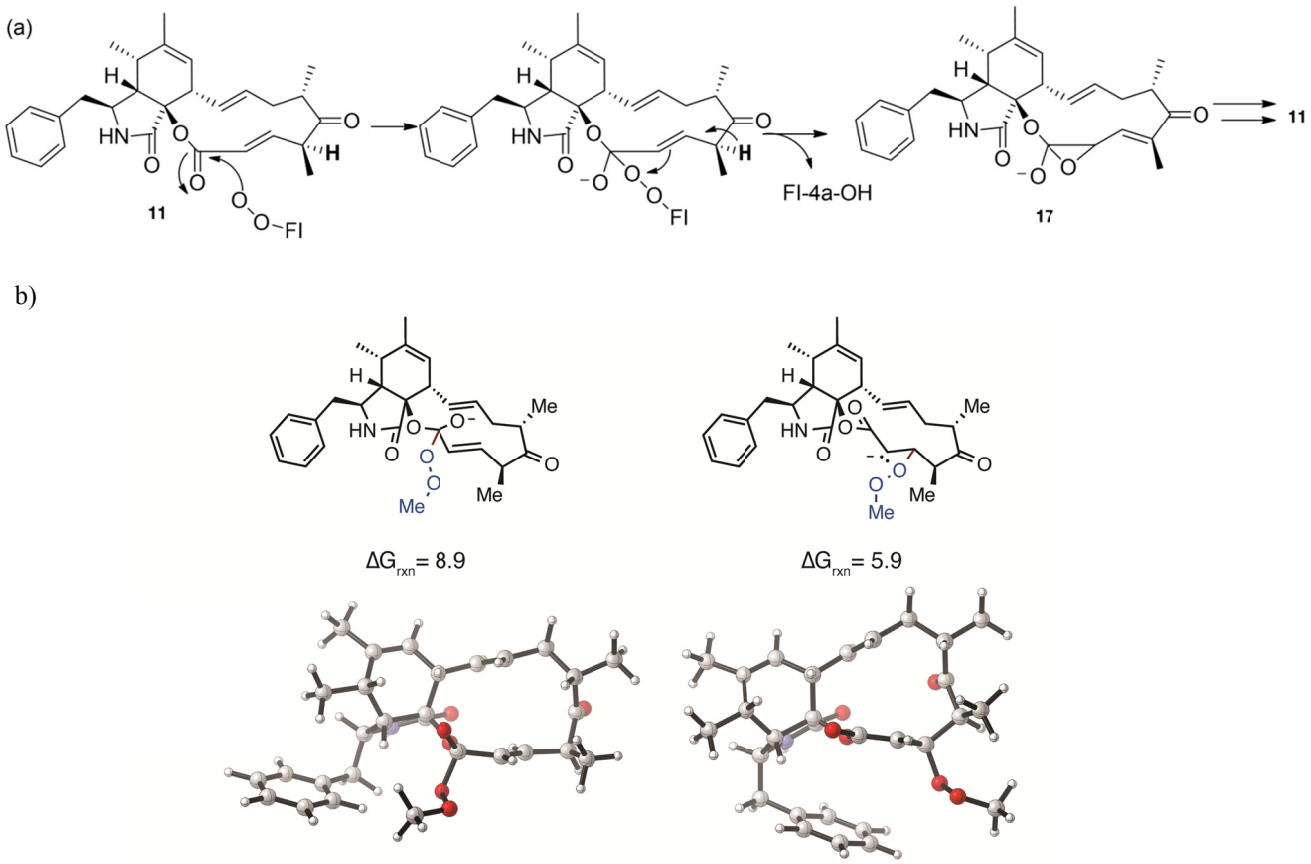

Supplementary Figure 32 (a) Alternative mechanism in conversion of **9** from **11** via **17**. An alternative mechanism in conversion from **11** to **9** may involve the direct (1,2) addition of the flavin-derived peroxide at the carbonyl carbon C21 of **11,** which can lead to the more facile formation of epoxy alkoxide **17. 17** can then convert to **9** as shown in **Supplementary Figure 31**. (b) Reaction free energies for the formation of the direct addition and Michael addition adducts of intermediate **11** and methyl hydroperoxide anion in kcal mol^{-1}. The Michael adduct is found to more stable by 3 kcal mol^{-1} .

In order to assess the likelihood of this mechanism, we modelled both the direct and Michael addition of **11** with methyl hydroperoxide anion. According to DFT calculation, the Michael adduct is to be 3 kcal mol^{-1} more stable than the product of direct addition. Furthermore, the effect of conjugated alkene in the α,β–unsaturated ester on the rate of direct addition was probed by comparing the model reaction of methyl crotonate and methyl hydroperoxide anion to that of the β,γ-unsaturated ester. Based on the activation energies shown in **Supplementary Figure 33**, the β,γ-unsaturated ester is roughly 100-fold more reactive than the α,β–unsaturated ester. This difference in reactivity is due to the resonance-donating ability of the alkene at the α,β position of the methyl crotonate, which renders the α,β–unsaturated ester less electrophilic at the carbonyl carbon. Hence, if the mechanism involved direct attack on ester carbonyl, one would expect the β,γ-unsaturated ester **8** to be more readily attacked. However, no conversion of **8** was observed in the presence of CcsB. Lastly, while the direct attack mechanism cannot be rigorously excluded, there are abundant examples from chemical synthesis showing that a peroxide attack on α−β unsaturated ester results in exclusive initial formation of the Michael adduct[33-36].

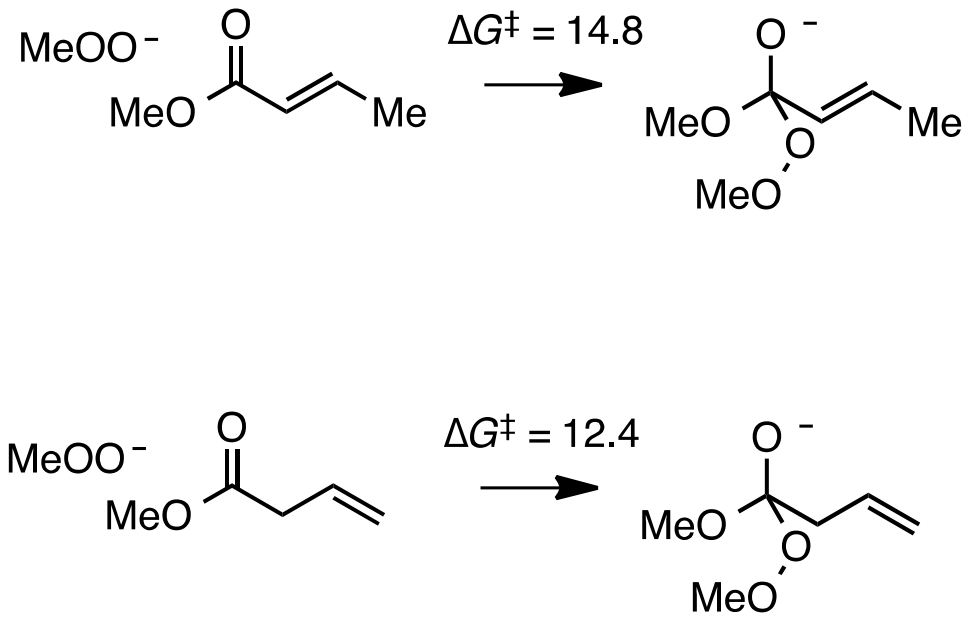

Supplementary Figure 33. Differences in the free energies of activation for the addition of methyl hydroperoxide anion to an α,β– and an β,γ–unsaturated ester. Energies reported in kcal mol^{-1} at 1 atm and 298.15 K. The calculation shows if direct addition to the ester were to take place, attack on β,γ–unsaturated ester (such as in **8**) is more favorable than an attack on an α,β–unsaturated ester (such as in **11**). In our reaction, compound **8** does not undergo the second oxidation.

Supplementary Note 1
Structure identification of compounds 7-9

1. Structure identification of 7.

The UV absorption spectrum of **7** is similar to that of **1**, suggesting it contains the same isoindolone scaffold. Its molecular weight was determined as 431 by ESI-MS *m/z* 432 $[M + H]^+$ and 454 $[M + Na]^+$ and the molecular formula of $C_{28}H_{33}NO_3$ was suggested by HRESIMS *m/z* 432.25183 $[M + H]^+$ (calcd for 432.25387, $C_{28}H_{34}NO_3$); 430.23815$[M - H]^-$(calcd for 430.23877, $C_{28}H_{32}NO_3$). ^{13}C NMR of **7** showed the C17 ketone (δ_C 210.2) and C1 amide (δ_C 173.4) were intact, which were supported by HMBC correlations from H22/H23 to C17, and from H3/H4 to C1. Most importantly, the carbonate at δ_C ~149.2 in **1** was shifted to δ_C 196.8 in **7** as would be expected for a ketone. The presence of an α,β-unsaturated ketone (C19-C21) was suggested by the chemical shifts (δ_C 196.8, 139.2, 135.2) and supported by HMBC correlations from H4/H8/H19/H20 to C21. Finally, to verify the structure of **7**, and determine stereochemistry of the C23 methyl substituent at C18, the crystal structure of **7** (named ketocytochalasin) was obtained as shown in **Supplementary Figure 12** (CCDC 970431).

2. Structure identification of 8.

The molecular weight of **8** was determined as 447 by ESI-MS *m/z* 448 $[M + H]^+$ and 470 $[M + Na]^+$ and the molecular formula of $C_{28}H_{34}NO_4$ was suggested by HRESIMS *m/z* 448.24674 $[M + H]^+$ (calcd for 448.24878, $C_{28}H_{34}NO_4$,); 446.23307$[M - H]^-$ (calcd for 446.23368, $C_{28}H_{32}NO_4$,).
The ^{13}C chemical shift of C9 at δ_C 86.6 and C21 at δ_C 170.8 in **8** suggested oxygen was inserted between C9 and C21 to form an ester. Unexpectedly, only four olefinic protons (H7, H13, H14, and H19) were identified, compared to the five present in **7**. In particular, the triplet C19 signal (δ_H 6.55) displayed new COSY (H19/H20 and H19/H23) and HMBC correlations (from H19 to C17 and C23) that indicates migration of the α,β-unsaturated double bond to form the vinylogous ketone at C17-C19 (δ_C 204.6, 143.3, and 132.5).

3. Structure identification of 9.

Complete NMR characterization of **9** verified the compound to be the carbonate-containing cytochalasin Z_{16}. While signals for the aliphatic ketone (δ_C 212.70, C17) and amide carbonyl (δ_C 170.2, C1) remained in the ^{13}C spectra, the vinylogous ketone signal in **7** (δ_C 196.8) disappeared, and instead a new signal (δ_C 149.8) corresponding to a carbonate carbonyl appeared. Also consistent with the carbonate structure of **9** is the shift of the adjacent quaternary C9 (δ_C from 68.9 to 89.0); and opposing shifts in the sp^2 C19 (δ_C 139.2 to 116.5) and C20 (δ_C 135.2 to 140.2) as a result of the neighbouring oxygen. The absolute structure of **9** was further confirmed by X-ray diffraction (**Supplementary Figure 20**, CCDC 970432).

Supplementary Note 2

Computational methods

All calculations were performed using Gaussian 09 (Revision D.01)[37]. Optimizations were performed using the M06-2X[38] hybrid-density functional with the 6-31+G(d,p) basis. The effects of solvation in water were taken into account by utilizing the SMD[39] implicit solvation model. An "ultrafine" integration grid consistent of 99 radial shells and 590 angular points per shell was employed. Frequency calculations were also performed using the SMD(H_2O)/M06-2X/6-31+G(d,p) model chemistry. Vibrational normal mode analysis confirmed nature of optimized stationary as either minima or transition states (first-order saddle points). Thermal corrections were determined assuming a standard state of 1 atm and 298.15 K. Errors in these corrections were mitigated by raising vibrational modes with frequency below 100 cm^{-1} to 100 cm^{-1}, as suggested by Truhlar[40]. All energies reported are Gibbs free energies in kcal mol^{-1}. The Cartesian Coordinates for Relevant DFT Structures are as follow.

Cartesian Coordinates for Relevant DFT Structures

MeOO-

C	1.06981	-0.21550	0.00001
H	1.10387	-0.85174	-0.89481
H	1.93505	0.45586	0.00016
H	1.10364	-0.85197	0.89465
O	-0.08023	0.59627	-0.00000
O	-1.23995	-0.27867	-0.00000

SCF energy: -190.306617 hartree
zero-point correction: +0.043378 hartree
enthalpy correction: +0.047958 hartree
free energy correction: +0.018637 hartree
quasiharmonic free energy correction: +0.018637 hartree

Methyl Crotonate

O	1.54084	-0.75658	-0.00001
C	0.56271	0.16020	-0.00001
O	0.79225	1.36095	-0.00002
C	-0.77185	-0.46463	-0.00004
C	2.88362	-0.24851	0.00003
H	3.52813	-1.12517	0.00011
H	3.05673	0.35283	0.89428
H	3.05682	0.35272	-0.89427
C	-1.87849	0.28707	0.00001
C	-3.26748	-0.25301	0.00002
H	-3.81121	0.11099	-0.87831
H	-3.81114	0.11086	0.87845
H	-3.27778	-1.34509	-0.00003
H	-1.76730	1.37117	0.00007
H	-0.81001	-1.55001	-0.00010

SCF energy: -345.657684 hartree
zero-point correction: +0.124186 hartree
enthalpy correction: +0.133218 hartree
free energy correction: +0.091645 hartree
quasiharmonic free energy correction: +0.091911 hartree

Model Direct Adduct

O	0.76121	-0.89990	-0.89228
C	-0.01124	-0.52870	0.26141
O	-0.19055	-1.47062	1.14285
C	-1.23680	0.16337	-0.31184
C	1.87189	-1.73611	-0.60105
H	2.47936	-1.77896	-1.50746
H	1.55161	-2.74873	-0.33716
H	2.47629	-1.32969	0.21729
C	-2.47343	-0.07749	0.12087
C	-3.70683	0.58762	-0.41093
H	-4.23023	1.12801	0.38548
H	-4.41109	-0.15406	-0.80349
H	-3.46647	1.29429	-1.20996
H	-1.06348	0.88299	-1.11045
H	-2.61201	-0.80596	0.92005
O	0.80480	0.51224	0.97868
O	1.06455	1.63690	0.13317
C	2.45117	1.63925	-0.17178
H	2.61653	2.56228	-0.73298
H	2.72386	0.77737	-0.78707
H	3.04688	1.65587	0.74632

SCF energy: -535.971483 hartree
zero-point correction: +0.169876 hartree
enthalpy correction: +0.182595 hartree
free energy correction: +0.132338 hartree
quasiharmonic free energy correction: +0.133084 hartree

Full Michael Adduct				Full Direct Adduct				Intermediate 8			
O	0.25207	0.20827	0.09921	O	0.34677	0.48627	0.58842	O	-0.00033	-0.45629	0.39241
C	-0.38366	0.21877	1.34786	C	0.69332	1.43795	-0.48223	O	0.07139	0.13592	-2.35796
C	-1.72840	0.51898	1.30430	C	2.16279	1.82644	-0.23002	C	1.27914	2.07944	-0.40473
H	-2.23294	0.57837	2.26266	H	2.61636	2.36415	-1.06608	H	1.39942	2.15639	-1.48511
C	-2.49999	0.76151	0.05748	C	2.87821	1.53357	0.85703	C	-0.81695	0.62183	-0.11309
H	-1.86355	0.57236	-0.81353	H	2.37631	1.05705	1.69830	O	-0.35426	0.04057	2.56388
C	-3.78276	-0.10153	-0.11259	C	4.38561	1.60292	0.99535	N	-2.18652	0.24383	-1.96659
H	-4.35923	0.36106	-0.92469	H	4.62191	1.78448	2.04925	H	-2.44516	-0.06032	-2.90054
C	-3.32276	-1.43885	-0.69635	C	4.81024	0.15299	0.78312	C	0.23391	-0.58404	1.70372
C	-3.52162	-2.74721	0.04705	C	5.24825	-0.35932	-0.58094	C	-0.89949	0.30202	-1.61524
H	-3.63585	-2.53824	1.11524	H	5.01270	0.39085	-1.34365	C	-2.72376	1.95982	0.97716
C	-2.31619	-3.67878	-0.15529	C	4.51967	-1.67692	-0.91781	H	-2.12286	2.08399	1.88989
H	-2.54091	-4.62002	0.36118	H	4.99644	-2.09567	-1.81402	C	-0.12253	1.99599	0.13679
H	-2.19926	-3.90257	-1.22115	H	4.66808	-2.39423	-0.10255	H	-0.05954	2.08443	1.22999
C	-1.05723	-3.07446	0.39191	C	3.05976	-1.45735	-1.17635	C	-1.04960	3.07355	-0.37959
H	-1.04990	-2.86641	1.46510	H	2.82372	-0.79191	-2.00645	C	-2.32762	3.07759	0.02465
C	0.00711	-2.72705	-0.33575	C	2.04754	-1.94975	-0.45373	C	4.67321	0.94928	0.36251
H	0.01424	-2.92250	-1.40815	H	2.26178	-2.59727	0.39713	H	4.55984	0.82915	1.44272
C	1.22107	-2.08127	0.27097	C	0.60257	-1.65570	-0.77600	C	2.35660	2.06454	0.38400
H	1.06617	-2.06345	1.35690	H	0.58738	-1.04833	-1.68758	H	2.21325	1.98933	1.46496
C	2.51575	-2.80697	-0.01839	C	-0.20521	-2.91763	-0.99279	C	-2.28798	0.60443	0.37438
C	3.65394	-2.32149	0.49766	C	-1.51419	-2.83269	-1.27337	H	-2.39491	-0.15299	1.15241
C	3.50995	-1.05139	1.32266	C	-2.08533	-1.42756	-1.31780	C	-3.13318	0.19270	-0.85931
H	2.86997	-1.29283	2.18425	H	-1.56837	-0.88867	-2.12636	H	-3.93205	0.91442	-1.04896
C	2.72338	-0.00791	0.49665	C	-1.68311	-0.68993	-0.02124	C	2.61938	-0.95771	1.40129
H	2.44956	0.80901	1.16507	H	-1.90106	0.37082	-0.16932	H	3.09579	-0.23637	2.05706
C	3.55111	0.54470	-0.69246	C	-2.41459	-1.19386	1.24410	C	3.09663	-1.15516	0.16071
H	4.55451	0.10910	-0.70662	H	-3.14077	-1.97661	1.00138	C	3.77889	2.13668	-0.09041
N	2.82822	0.07851	-1.86984	N	-1.34709	-1.76597	2.05907	H	3.81215	2.20888	-1.18438
H	3.09586	0.35773	-2.80858	H	-1.52371	-2.21118	2.95335	H	4.24796	3.04278	0.31315
C	1.61704	-0.43311	-1.63778	C	-0.10562	-1.47458	1.66572	C	-2.74662	-2.27371	-0.40030
C	1.41636	-0.58337	-0.11967	C	-0.17116	-0.79559	0.28837	C	-3.76420	-1.20859	-0.72890
O	0.32302	-0.02841	2.37489	O	0.38277	1.14451	-1.66750	H	-4.27567	-1.44237	-1.66926
C	-4.66471	-0.21841	1.12950	C	5.08322	2.62280	0.10708	H	-4.52260	-1.15493	0.05967
H	-5.06878	0.75760	1.40594	H	4.82875	3.62871	0.45382	C	-1.90988	-2.79780	-1.39456
H	-4.10976	-0.60498	1.98795	H	4.79006	2.54332	-0.94298	H	-2.04373	-2.48695	-2.42784
H	-5.51121	-0.88592	0.94358	H	6.16945	2.50219	0.16268	C	1.36165	-1.56662	1.96174
O	-2.80647	-1.44582	-1.80797	O	4.89310	-0.58622	1.75777	H	1.10879	-2.51539	1.48341
C	-4.81066	-3.39949	-0.47987	C	6.76949	-0.57221	-0.53353	H	1.43460	-1.70847	3.04022
H	-5.00142	-4.32850	0.06449	H	7.12843	-0.89189	-1.51539	C	-4.18818	1.94451	1.40996
H	-4.70165	-3.63611	-1.54315	H	7.02682	-1.34501	0.19709	H	-4.36953	1.09741	2.07944
H	-5.67953	-2.74623	-0.36022	H	7.29381	0.34813	-0.25545	H	-4.44010	2.85956	1.95315
C	5.00020	-2.94670	0.27626	C	-2.39187	-4.03057	-1.50245	H	-4.87814	1.86140	0.56512
C	4.80784	-0.47610	1.88647	C	-3.58260	-1.32565	-1.61157	C	-2.56451	-2.70612	0.91964
H	5.28566	-1.18932	2.56419	H	-3.80026	-1.69473	-2.61868	H	-3.21150	-2.31479	1.70164
H	4.59434	0.43413	2.45650	H	-3.90933	-0.27953	-1.56458	C	4.21098	-0.30610	-0.36028
H	5.53238	-0.22300	1.10655	H	-4.19292	-1.89999	-0.90870	C	-1.56452	-3.62333	1.24297
C	3.70321	2.07839	-0.68950	C	-3.11686	-0.05709	2.01262	H	-1.43669	-3.94207	2.27350
H	4.36844	2.33733	0.14144	H	-3.50798	-0.46168	2.95294	C	2.52823	-2.13104	-0.83144
H	4.20256	2.37460	-1.61924	H	-2.36190	0.70042	2.25320	H	1.80220	-2.80374	-0.37417
C	2.38919	2.80358	-0.53948	C	-4.22834	0.56566	1.20719	H	2.02902	-1.59712	-1.64850
C	1.98262	3.28364	0.71186	C	-5.44381	-0.10523	1.03212	H	3.32812	-2.72955	-1.27555
H	2.65007	3.17627	1.56407	H	-5.60773	-1.05497	1.53612	O	4.69445	-0.57521	-1.45905
C	0.73727	3.88908	0.87939	C	-6.43695	0.42658	0.21134	C	-0.90500	-3.71138	-1.07550
H	0.43935	4.25180	1.85878	H	-7.37347	-0.10824	0.08335	H	-0.26094	-4.10011	-1.85907
C	-0.12148	4.02799	-0.21081	C	-6.23055	1.64076	-0.44700	C	-0.72718	-4.12448	0.24551
H	-1.09235	4.49725	-0.08378	H	-7.00418	2.05042	-1.08904	H	0.05860	-4.83153	0.49547

C	0.27233	3.55856	-1.46474
H	-0.39180	3.66383	-2.31775
C	1.51991	2.95531	-1.62732
H	1.82176	2.59811	-2.60905
O	0.77862	-0.72751	-2.49846
H	5.46810	-3.22934	1.22600
H	4.91418	-3.84117	-0.34618
H	2.49900	-3.70168	-0.63856
H	5.68310	-2.24510	-0.21684
O	-2.81639	2.16260	-0.18683
O	-3.55836	2.67875	0.92444
C	-4.76005	3.21366	0.39183
H	-5.31329	3.58653	1.25717
H	-4.54606	4.03929	-0.29408
H	-5.34179	2.43993	-0.11979

SCF energy: -1632.318695 hartree
zero-point correction: +0.609048 hartree
enthalpy correction: +0.643968 hartree
free energy correction: +0.545558 hartree
quasiharmonic free energy correction: +0.551235 hartree

C	-5.02850	2.32785	-0.26551
H	-4.86118	3.27777	-0.76564
C	-4.03870	1.79293	0.55879
H	-3.10310	2.33201	0.70514
O	0.93354	-1.75015	2.28243
H	-2.86085	-3.99994	-2.49174
H	-1.81108	-4.95371	-1.42628
H	0.29902	-3.88030	-0.92673
H	-3.20028	-4.07178	-0.76337
O	-0.19243	2.54515	0.12943
O	0.05039	3.76016	-0.61168
C	-0.93683	3.80995	-1.62435
H	-0.75558	3.03788	-2.38607
H	-1.94161	3.69831	-1.19688
H	-0.83767	4.81048	-2.05756

SCF energy: -1632.312006 hartree
zero-point correction: +0.607512 hartree
enthalpy correction: +0.642860 hartree
free energy correction: +0.543266 hartree
quasiharmonic free energy correction: +0.549194 hartree

C	6.13757	1.24704	0.04951
H	6.27349	1.47680	-1.01099
H	6.46894	2.11102	0.63186
H	6.77784	0.39639	0.30018
H	-0.65953	3.81944	-1.06934
C	-3.33431	4.09668	-0.42162
H	-3.75371	4.63871	0.43324
H	-2.87716	4.82080	-1.10075
H	-4.17461	3.61877	-0.93824

SCF energy: -1442.006356 hartree
zero-point correction: +0.562469 hartree
enthalpy correction: +0.593628 hartree
free energy correction: +0.503919 hartree
quasiharmonic free energy correction: +0.507856 hartree

Intermediate 11							
O	-0.11932	0.47049	-0.14566	O	4.55316	-0.16739	1.84406
C	0.43591	0.55661	-1.36332	C	5.80014	-1.87042	-0.21053
C	1.82231	1.06650	-1.32575	H	5.88362	-2.72203	-0.89067
H	2.29576	1.20928	-2.29229	H	6.07065	-2.20198	0.79673
C	2.47796	1.13681	-0.16128	H	6.51511	-1.10413	-0.52595
H	1.92004	0.95966	0.75749	C	-3.95878	-3.70716	0.11888
C	3.96154	1.26684	0.02229	C	-4.40159	-1.47533	-1.75996
H	4.15375	2.00950	0.80387	H	-4.66939	-2.34516	-2.36616
C	4.32684	-0.08868	0.64624	H	-4.43763	-0.59245	-2.40656
C	4.36284	-1.33336	-0.22710	H	-5.16948	-1.36104	-0.98958
H	4.09456	-1.06115	-1.25315	C	-3.76252	1.70364	0.44005
C	3.36189	-2.40383	0.27114	H	-4.40234	1.80219	-0.44338
H	3.71765	-3.36691	-0.11736	H	-4.34865	2.00777	1.31452
H	3.38985	-2.46487	1.36485	C	-2.53617	2.57057	0.29482
C	1.95984	-2.18433	-0.22481	C	-2.08968	2.97209	-0.97050
H	1.86946	-2.03167	-1.30430	H	-2.68237	2.72257	-1.84780
C	0.84342	-2.17477	0.50971	C	-0.89055	3.66905	-1.12054
H	0.89491	-2.32383	1.58775	H	-0.55691	3.96224	-2.11187
C	-0.51391	-1.95391	-0.10978	C	-0.11912	3.98190	-0.00059
H	-0.38208	-2.00769	-1.19925	H	0.81957	4.51574	-0.11543
C	-1.57813	-2.94858	0.29096	C	-0.56451	3.60997	1.26853
C	-2.80995	-2.80316	-0.21923	H	0.02353	3.85920	2.14696
C	-2.99834	-1.63664	-1.17922	C	-1.76476	2.91338	1.41323
H	-2.32411	-1.81425	-2.03011	H	-2.10323	2.62587	2.40596
C	-2.48375	-0.33175	-0.52308	O	-0.50333	-0.34209	2.53143
H	-2.39034	0.41782	-1.31075	H	-4.36885	-4.18085	-0.77992
C	-3.41511	0.20723	0.59324	H	-3.64351	-4.49132	0.81187
H	-4.34969	-0.35727	0.63712	H	-1.33091	-3.74278	0.99251
N	-2.66347	-0.03956	1.81862	H	-4.77665	-3.14329	0.58225
H	-3.00752	0.26538	2.72406				
C	-1.36482	-0.29873	1.64817	SCF energy: -1441.995987 hartree			
C	-1.10308	-0.53487	0.15071	zero-point correction: +0.561736 hartree			
O	-0.11539	0.17851	-2.38415	enthalpy correction: +0.593270 hartree			
C	4.75816	1.59729	-1.23593	free energy correction: +0.501801 hartree			
H	4.44549	2.57147	-1.62246	quasiharmonic free energy correction:			
H	4.61137	0.85801	-2.02759	+0.506961 hartree			
H	5.82523	1.64831	-1.00538				

Model Michael Adduct				**Model Direct Addition Transition State**				**Model Michael Transition State**			
O	-2.76657	-0.70347	-0.01744	C	2.40381	-1.73881	0.04136	O	2.27068	-0.54143	-0.61971
C	-1.41151	-0.56317	0.27867	O	1.07958	-1.60105	-0.46858	C	1.19370	-0.42335	0.21288
O	-0.91233	-1.63042	0.76391	H	2.91268	-2.43682	-0.62281	O	1.27378	0.27177	1.23434
C	-0.76298	0.63128	0.05007	H	2.39155	-2.13696	1.05879	C	0.06715	-1.18058	-0.24329
C	-3.46789	0.40695	-0.56041	H	2.91832	-0.77327	0.03141	C	3.44053	0.19494	-0.25664
H	-4.49576	0.07473	-0.70953	C	0.29587	-0.67942	0.18721	H	4.17696	-0.02286	-1.02895
H	-3.04216	0.71128	-1.52193	C	-1.07343	-0.68723	-0.40105	H	3.81579	-0.12575	0.71784
H	-3.45770	1.25654	0.13002	O	0.54943	-0.34502	1.35331	H	3.22912	1.26668	-0.23449
C	0.68385	0.74458	0.35338	O	0.95349	0.88065	-0.95203	C	-1.14987	-1.08856	0.38843
C	1.15668	2.17706	0.53544	O	1.29914	1.96433	-0.08398	C	-2.25480	-2.06254	0.11971
H	2.24297	2.22497	0.64709	C	0.12692	2.70697	0.18289	H	-3.23397	-1.61932	0.31675
H	0.70173	2.60745	1.43224	H	0.42797	3.54726	0.81603	H	-2.14236	-2.92915	0.78170
H	0.86463	2.78555	-0.32696	H	-0.61582	2.09805	0.71082	H	-2.22371	-2.41725	-0.91412
O	1.38889	0.14244	-0.78656	H	-0.31023	3.08747	-0.74900	O	-2.23764	0.47203	-0.44681
O	2.76838	-0.04438	-0.43347	C	-2.16039	-0.46198	0.33824	O	-1.29864	1.49419	-0.78167
C	2.92114	-1.41664	-0.09949	H	-1.14378	-0.90950	-1.46351	C	-1.17794	2.36328	0.32481
H	0.96012	0.13350	1.22257	H	-2.03036	-0.24852	1.39958	H	-1.17528	-0.58616	1.35245
H	-1.26318	1.48176	-0.39383	C	-3.56117	-0.47310	-0.18716	H	0.17948	-1.74899	-1.16138
H	3.97394	-1.53433	0.16794	H	-3.58430	-0.69301	-1.25762	H	-0.42031	3.10595	0.05647
H	2.68317	-2.05071	-0.95895	H	-4.04336	0.49633	-0.01968	H	-0.85319	1.81763	1.21868
H	2.28966	-1.68447	0.75386	H	-4.16537	-1.22097	0.33742	H	-2.13063	2.86752	0.53046
SCF energy: -535.977531 hartree zero-point correction: +0.171044 hartree enthalpy correction: +0.183664 hartree free energy correction: +0.132669 hartree quasiharmonic free energy correction: +0.134233 hartree				SCF energy: -535.960177 hartree zero-point correction: +0.168551 hartree enthalpy correction: +0.181521 hartree free energy correction: +0.130405 hartree quasiharmonic free energy correction: +0.131164 hartree				SCF energy: -535.955997 hartree zero-point correction: +0.169138 hartree enthalpy correction: +0.181850 hartree free energy correction: +0.131108 hartree quasiharmonic free energy correction: +0.132144 hartree			

Supplementary Note 3

Synthesis procedures for cytochalasin D derivative dehydrozygosporin D (12)

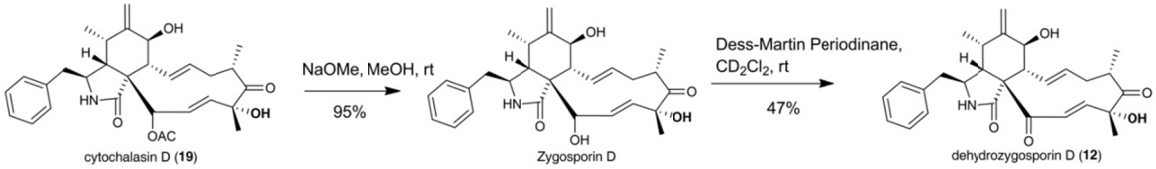

1. Isolation of cytochalasin D (19). The producer organism, *Zygosporium masonii*, was obtained from the University of Alberta Microfungus Collection and Herbarium (UAMH) as a frozen mycelia suspension (1 mL). This was thawed, and transferred to a potato-dextrose-agar (PDA) petri dish (~10 mL), and maintained at room temperature for several days. Upon sporulation of the organism on solid media, a swab of the spores was transferred into freshly autoclaved potato-dextrose (PD) liquid medium (2 × 25 mL in 125 mL flasks). These were incubated at 27 °C, with shaking at 225 rpm for seven days, at which point white spheres (~ 50) representing the organism were observed in the flask. These were transferred sterilely into large-scale production flasks (2×500 mL) containing autoclaved PD and shaken at 225 rpm and 27°C for 10-12 days. The cultures (including media) were pulverized in a Waring blender and then stirred with an equal volume of ethyl acetate (EtOAc) for 2h at 4 °C. This mixture was filtered through cheesecloth, and the organic and aqueous layers were separated. The aqueous layer was washed with one volume of EtOAc, and the combined organic layers were dried with brine (one volume) and then over Na_2SO_4. The drying agent was filtered and the organic layer was evaporated to give crude extract. For larger amounts of crude extract, cytochalasin D could be crystallized directly from acetone. Smaller amounts were purified by consecutive columns of silica-gel chromatography, eluted by 97:3 CH_2Cl_2:MeOH followed by 1:1 EtOAc : hexanes. The title product was isolated as a white solid (31-70 mg/L yield), and spectra were consistent with literature.

Cytochalasin D (**19**): white solid; $[\alpha]_D$ -31.34° (*c* = 4.90, $CHCl_3$). IR (film) ν (cm^{-1}): 3416.4, 2969.5, 2932.8, 1739.6, 1702.8, 1690.8. ^{1}H-NMR (600 MHz, $CDCl_3$): δ (ppm) 7.31 (d, 2H, *J* = 7.6 Hz), 7.26 (s, 1H), 7.24 (s, 1H), 7.14-7.12 (m, 2H), 6.11 (dd, 1H, *J* = 15.8, 2.7 Hz), 5.69 (dd, 1H, *J* = 15.6, 9.8 Hz), 5.63 (app t, 1H, *J* = 2.5 Hz), 5.50 (s, 1H), 5.36-5.30 (ddd, 1H, *J* = 15.8, 10.2, 5.2 Hz), 5.29 (d, 1H, *J* = 1.7 Hz), 5.14 (dd, 1H, *J* = 15.8, 2.3 Hz), 5.08 (s, 1H), 4.62 (br s, 1H), 3.81 (dd, 1H, *J* = 10.5, 0.8 Hz), 3.23 (dt, 1H, *J* = 8.8, 4.2 Hz), 2.87-2.79 (m, 2H), 2.75-2.71 (m, 2H), 2.67 (dd, 1H, *J* = 13.4, 9.4 Hz), 2.51 (app q, 1H, *J* = 11.3 Hz), 2.25 (s, 3H), 2.15 (dd, 1H, *J* = 5.1, 3.4 Hz), 2.03-2.00 (m, 1H), 1.50 (s, 3H), 1.19 (d, 3H, *J* = 6.9 Hz), 0.95 (d, 3H, *J* = 6.7 Hz). ^{13}C-NMR (125 MHz, $CDCl_3$): δ (ppm) 210.2, 173.6, 169.7, 147.6, 137.3, 134.3, 134.1, 132.3, 130.7, 129.1, 129.0, 127.6, 127.1, 114.5, 77.7, 69.9, 53.5, 53.3, 50.1, 47.0, 45.4, 42.4, 37.8, 32.7, 29.7, 24.2, 20.8, 19.4, 13.7. HRESI-MS (calculated): 508.2694 $[M+H]^+$; (observed): 508.2694 $[M+H]^+$.

2. Desacetylation of cytochalasin D to give Zygosporin D

A fresh solution of NaOMe in methanol (1M) was prepared by dissolving hexanes-washed sodium (23 mg) in dry methanol (1 mL) at 0 °C. To a solution of cytochalasin D (41 mg, 0.081 mmol) in dry methanol (2 mL) was added NaOMe (45 mL of 1M solution), which was stirred at room temperature for 2-3 hours. Progress of the deprotection reaction was monitored by TLC (95:5 CH_2Cl_2: MeOH). When hydrolysis of the acetyl group was deemed complete, the mixture was quenched with an equal amount of HCl (45 ml of a 1M solution) and the solvent was removed under reduced pressure. The residue was taken up in $CDCl_3$, dried over Na_2SO_4 and analyzed by NMR. Typical yields of 92-97% were observed, and the product Zygosporin D was directly used in the following step without further purification.

Zygosporin D: $[\alpha]_D$ -21.51 ° (*c* = 4.80, $CHCl_3$). IR (film) ν (cm^{-1}): 3400.1, 3086.0, 3062.2, 2967.9, 2932.4, 2851.8, 1700.5, 1686.6.^{1}H-NMR (500 MHz, $CDCl_3$): δ (ppm) 7.35 (t, 2H, *J*=7.3 Hz), 7.25-7.23 (m, 1H), 7.16 (d, 2H, *J*=7.0 Hz), 6.26 (dd, 1H, *J* = 15.9, 2.6 Hz), 5.71 (dd, 1H, *J* = 15.8, 9.0 Hz), 5.45 (dd, 1H, *J* = 15.9, 2.3 Hz), 5.38 (br s, 1H), 5.36-5.32 (m, 1H), 5.31 (ddd, 1H, *J* = 15.3, 10.2, 4.8 Hz), 5.17-5.12 (m, 1H), 4.67 (br s, 1H), 4.14-4.10 (m, 1H), 3.83 (d, 1H, *J* = 11.2 Hz), 3.23 (app dt, 1H, *J* = 8.7, 4.1 Hz), 2.97-2.90 (m, 2H), 2.87 (app t, 1H, *J* = 10.2 Hz), 2.81-2.72 (m, 1H), 2.65-2.58 (m, 2H), 2.53 (app q, 1H, *J* = 11.9 Hz), 2.05 (dd, 1H, *J* = 13.0, 5.2 Hz), 1.58 (s, 3H), 1.23 (d, 3H, *J* = 6.9 Hz), 1.15 (d, 3H, *J* = 6.7 Hz). ^{13}C-NMR (100 MHz, $CDCl_3$): δ (ppm) 210.2, 174.9, 148.1, 137.3, 137.0, 133.7, 131.1, 129.2, 128.9, 127.2, 127.1, 114.1, 77.8, 76.6, 69.7, 54.2, 53.5, 50.2, 45.7, 45.4, 42.4, 37.7, 32.9, 24.3, 19.4, 13.9. HRESI-MS (calculated): 488.2407 $[M+Na]^+$; (observed): 488.2399 $[M+Na]^+$.

3. Synthesis of Dehydrozygosporin D (12)

To avoid over oxidation during this reaction, careful NMR analysis was used to monitor reaction progress. Specifically, the doublets corresponding to the hydrogen atoms attached to C20 and C19 of the starting material (6.22 and 5.45 ppm respectively) were followed. In the desired product these peaks shifted to 6.97 and 6.35 ppm. Over-oxidation resulted in a slight upfield shift of these signals. Zygosporin D (19 mg, 0.04 mmol) was dissolved in CD_2Cl_2 (2 mL), in a dried round bottom flask (5 mL). A solution of Dess-Martin periodinane (17 mg, 0.04 mmol) in CD_2Cl_2 (1 mL) was also prepared. Aliquots (0.1-0.2 mL) of the periodinane were added to Zygosporin D and stirred at room temperature. The reaction progress was monitored by NMR spectroscopy every 30-60 minutes, and more periodinane was added until reaction progress showed 50-65% completion (further reaction resulted in doubly-oxidized product which is difficult to separate). The reaction was quenched with isopropanol (0.5 mL) and evaporated under reduced pressure. The residue was directly purified by silica gel chromatography, using an eluent of 1:1 hexanes:EtOAc. The title product was obtained as a white solid (8.7 mg, 47%).

Dehydrozygosporin D (**12)**: white solid; $[\alpha]_D$ -40.22° (*c* = 0.87, $CHCl_3$). IR (film) ν (cm^{-1}): 3417.2, 3292.0, 2969.1, 2933.7, 1685.6, 1619.3, 1454.1, 1375.2, 1015.6, 754.9^{1}H-NMR (600 MHz, $CDCl_3$): δ (ppm) 7.32 (t, 2H, *J*=7.5 Hz), 7.25 (t, 1H, *J*=7.4 Hz), 7.12 (d, 2H, *J*=7.0 Hz), 6.97 (d, 1H, *J*=15.7 Hz), 6.35 (d, 1H, *J*=15.7 Hz), 5.80 (ddd, 1H, *J*=15.5, 9.8, 0.9 Hz), 5.58 (br s, 1H), 5.25 (s, 1H), 5.19 (ddd, 1H, *J*=15.5, 10.9, 4.7), 5.08 (s, 1H), 4.71 (br s, 1H), 4.06 (d, 1H, *J*=10.1 Hz), 3.34-3.28 (m, 1H), 3.24 (dd, 1H, *J*=5.9, 2.4 Hz), 2.83-2.75 (m, 1H), 2.72 (ddd, 1H, *J*=10.9, 6.8, 1.3 Hz), 2.67 (dd, 1H, *J*=13.4, 5.5 Hz), 2.57 (dt, 1H, *J*=13.1, 11.0 Hz), 2.46 (dd, 1H, *J*=13.3, 8.9 Hz), 2.41 (app t, 1H, *J*=9.9 Hz), 2.12-2.07 (m, 1H), 1.64 (s, 3H), 1.21 (d, 3H, *J*=6.8 Hz), 1.00 (d, 3H, *J*=6.7 Hz). ^{13}C-NMR (125 MHz, $CDCl_3$): δ (ppm) 209.9, 197.4, 172.7, 148.5, 143.3, 137.0, 135.0, 134.3, 129.8, 129.3, 128.9, 127.0, 114.4, 78.6, 71.5, 64.1, 53.1, 51.7, 45.2, 44.2, 42.9, 38.3, 31.6, 23.6, 19.8, 13.0. HRESI-MS (calculated): 486.2241 $[M+Na]^+$; (observed): 486.2251 $[M+Na]^+$.

Supplementary Data Set List

Data set 1: CIF file for the crystal structure of cytochalasin Z_{16} (**9**), CCDC 970432

Data set 2: CIF file for the crystal structure of ketocytochalasin (**7**), CCDC 970431

Data set 3: Checkcif output file for CIF file of **9.**

Data set 4: Checkcif output file for CIF file of **7.**

Supplementary References

1. Lin, Z.J. et al. Bioactive Cytochalasins from Aspergillus flavipes, an Endophytic Fungus Associated with the Mangrove Plant Acanthus ilicifolius. *Helv Chim Acta* **92**, 1538-1544 (2009).
2. Fedorova, N.D. et al. Genomic islands in the pathogenic filamentous fungus Aspergillus fumigatus. *Plos Genet* **4**, e1000046 (2008).
3. Udagawa, T. et al. Cytochalasin E, an epoxide containing Aspergillus-derived fungal metabolite, inhibits angiogenesis and tumor growth. *J Pharmacol Exp Ther* **294**, 421-427 (2000).
4. Buchi, G. et al. Structure of Cytochalasin-E, a Toxic Metabolite of Aspergillus-Clavatus. *J Am Chem Soc* **95**, 5423-5425 (1973).
5. Takamatsu, S., Zhang, Q.L., Schrader, K.K., ElSohly, H.N. & Walker, L.A. Characterization of Mycotypha metabolites found to be inhibitors of cell adhesion molecules. *J Antibiot* **55**, 585-592 (2002).
6. Namatame, I., Tomoda, H., Arai, M. & Omura, S. Effect of fungal metabolites cytochalasans on lipid droplet formation in mouse macrophages. *J Antibiot* **53**, 19-25 (2000).
7. Pongcharoen, W., Rukachaisirikul, V., Phongpaichit, S., Rungjindamai, N. & Sakayaroj, J. Pimarane diterpene and cytochalasin derivatives from the endophytic fungus Eutypella scoparia PSU-D44. *J Nat Prod* **69**, 856-858 (2006).
8. Mejia-Oneto, J.M. & Padwa, A. Total synthesis of the alkaloid (+/-)-aspidophytine based on carbonyl ylide cycloaddition chemistry. *Helv Chim Acta* **91**, 285-302 (2008).
9. Haidle, A.M. & Myers, A.G. An enantioselective, modular, and general route to the cytochalasins: Synthesis of L-696,474 and cytochalasin B. *P Natl Acad Sci USA* **101**, 12048-12053 (2004).
10. Thomas, E.J. & Whitehead, J.W.F. Cytochalasan Synthesis - Total Synthesis of Cytochalasin-H. *J Chem Soc Perk T 1*, 507-518 (1989).
11. Dyke, H., Sauter, R., Steel, P. & Thomas, E.J. Cytochalasan Synthesis - Total Synthesis of Cytochalasin-G. *J Chem Soc Chem Comm*, 1447-1449 (1986).
12. Liu, R. et al. Novel open-chain cytochalasins from the marine-derived fungus Spicaria elegans. *J Nat Prod* **71**, 1127-1132 (2008).
13. Liu, R. et al. 10-phenyl-[12]-cytochalasins Z(7), Z(8), and Z(9) from the marine-derived fungus Spicaria elegans. *J Nat Prod* **69**, 871-875 (2006).
14. Wang, F.Z. et al. Three New Cytochalasins from the Marine-Derived Fungus Spicaria elegans KLA03 by Supplementing the Cultures with L- and D-Tryptophan. *Chem Biodivers* **8**, 887-894 (2011).
15. Zheng, C.J. et al. Bioactive Phenylalanine Derivatives and Cytochalasins from the Soft Coral-Derived Fungus, Aspergillus elegans. *Mar Drugs* **11**, 2054-2068 (2013).
16. Lin, Z.J., Zhu, T.J., Zhang, G.J., Wei, H.J. & Gu, Q.Q. Deoxy-cytochalasins from a marine-derived fungus Spicaria elegans. *Can J Chem* **87**, 486-489 (2009).
17. Buchanan, M.S., Hashimoto, T. & Asakawa, Y. Cytochalasins from a Daldinia sp of fungus. *Phytochemistry* **41**, 821-828 (1996).
18. Kimura, Y., Nakajima, H. & Hamasaki, T. Structure of Rosellichalasin, a New Metabolite Produced by Rosellinia-Necatrix. *Agr Biol Chem Tokyo* **53**, 1699-1701 (1989).
19. Tomikawa, T. et al. Structure of aspochalasin H, a new member of the aspochalasin family. *J Antibiot* **55**, 666-668 (2002).
20. Gebhardt, K. et al. Aspochalamins A-D and aspochalasin Z produced by the endosymbiotic fungus Aspergillus niveus LU 9575 - I. Taxonomy, fermentation, isolation and biological activities. *J Antibiot* **57**, 707-714 (2004).

21. Wagenaar, M.M., Corwin, J., Strobel, G. & Clardy, J. Three new cytochalasins produced by an endophytic fungus in the genus Rhinocladiella. *J Nat Prod* **63**, 1692-1695 (2000).
22. Liu, J.L., Hu, Z.Y., Huang, H.Y., Zheng, Z.H. & Xu, Q.Y. Aspochalasin U, a moderate TNF-alpha inhibitor from Aspergillus sp. *J Antibiot* **65**, 49-52 (2012).
23. Jayasuriya, H. et al. Isolation and structure of antagonists of chemokine receptor (CCR5). *J Nat Prod* **67**, 1036-1038 (2004).
24. Abate, D., Abraham, W.R. & Meyer, H. Cytochalasins and phytotoxins from the fungus Xylaria obovata. *Phytochemistry* **44**, 1443-1448 (1997).
25. Zhang, Y.G. et al. Alachalasins A-G, new cytochalasins from the fungus Stachybotrys charatum. *Bioorgan Med Chem* **16**, 2627-2634 (2008).
26. Vederas, J.C. Structural Dependence of O-18-Isotope Shifts in C-13-Nmr Spectra. *J Am Chem Soc* **102**, 374-376 (1980).
27. Vederas, J.C. & Nakashima, T.T. Biosynthesis of Averufin by Aspergillus-Parasiticus - Detection of O-18-Label by C-13-Nmr Isotope Shifts. *J Chem Soc Chem Comm*, 183-185 (1980).
28. Zhang, H.W. et al. Ardeemins and Cytochalasins from Aspergillus terreus Residing in Artemisia annua. *Planta Med* **76**, 1616-1621 (2010).
29. Espada, A., RiveraSagredo, A., delaFuente, J.M., HuesoRodriguez, J.A. & Elson, S.W. New cytochalasins from the fungus Xylaria hypoxylon. *Tetrahedron* **53**, 6485-6492 (1997).
30. Rubin, M.B. & Inbar, S. Thermal and Base-Catalyzed Rearrangements of Diacyl Carbinols. *Tetrahedron Lett*, 5021-5024 (1979).
31. Rubin, M.B. & Inbar, S. Equilibria among Anions of Alpha-Hydroxy Beta-Diketones and Alpha-Ketol Esters. *J Org Chem* **53**, 3355-3358 (1988).
32. Hong, X.C., Mejia-Oneto, J.M. & Padwa, A. Lewis acid-promoted alpha-hydroxy beta-dicarbonyl to alpha-ketol ester rearrangement. *Tetrahedron Lett* **47**, 8387-8390 (2006).
33. Gonzalez, F.V., Izquierdo, J., Rodriguez, S., McKerrow, J.H. & Hansell, E. Dipeptidyl-alpha,beta-epoxyesters as potent irreversible inhibitors of the cysteine proteases cruzain and rhodesain. *Bioorg Med Chem Lett* **17**, 6697-6700 (2007).
34. Rodriguez, S. et al. Diastereoselective synthesis of gamma-hydroxy alpha,beta-epoxyesters and their conversion into beta-hydroxy alpha-sulfenyl gamma-butyrolactones. *Tetrahedron* **62**, 11112-11123 (2006).
35. Cefalo, D.R. et al. Enantioselective synthesis of unsaturated cyclic tertiary ethers by Mo-catalyzed olefin metathesis. *J Am Chem Soc* **123**, 3139-3140 (2001).
36. Cusso, O., Garcia-Bosch, I., Ribas, X., Lloret-Fillol, J. & Costas, M. Asymmetric Epoxidation with H2O2 by Manipulating the Electronic Properties of Non-heme Iron Catalysts. *J Am Chem Soc* **135**, 14871-14878 (2013).
37. Tobin, S.J. & Foresman, J.B. Student exploration of the Mills-Nixon effect: Kinetics measurements using FT-NMR and electronic structure calculations using Gaussian 09. *Abstr Pap Am Chem S* **241** (2011).
38. Zhao, Y. & Truhlar, D.G. The M06 suite of density functionals for main group thermochemistry, thermochemical kinetics, noncovalent interactions, excited states, and transition elements: two new functionals and systematic testing of four M06-class functionals and 12 other functionals. *Theor Chem Acc* **120**, 215-241 (2008).
39. Marenich, A.V., Cramer, C.J. & Truhlar, D.G. Universal Solvation Model Based on Solute Electron Density and on a Continuum Model of the Solvent Defined by the Bulk Dielectric Constant and Atomic Surface Tensions. *J Phys Chem B* **113**, 6378-6396 (2009).
40. Ribeiro, R.F., Marenich, A.V., Cramer, C.J. & Truhlar, D.G. Use of Solution-Phase Vibrational Frequencies in Continuum Models for the Free Energy of Solvation. *J Phys Chem B* **115**, 14556-14562 (2011).